Non-adiabatic energization and transport of planetary ions in the magnetospheric flanks of Mercury

Sae Aizawa[1]; Dominique Delcourt[2]; Naoki Terada[3]
[1] Geophysics, Tohoku Univ; [2] LPP, Ecole Polytechnique, CNRS; [3] Dept. Geophys., Grad. Sch. Sci., Tohoku Univ.

We investigate the acceleration and transport of planetary ions within Kelvin-Helmholtz (KH) vortices that develop in the magnetospheric flanks of Mercury, using single-particle trajectory calculations in a field model obtained from MHD simulations. Due to the presence of heavy ions of planetary origin (e.g., O^+, Na^+, and K^+) following ionization of exospheric neutrals and due to the complicated field structure during the KH vortex development, the scale of electric field variation may be comparable with ion gyration motion. Therefore, ions may experience non-adiabatic energization as they drift across the magnetopause. In this study, we consider realistic configurations for both dawn and dusk magnetospheric flanks, and we focus on the effect of the spatial and temporal variations of the electric field magnitude and orientation along the ion path on the ion dynamics. We show that the intensification rather than the change of orientation is responsible for large non-adiabatic energization of heavy ions of planetary origin. This energization systematically occurs for ions with low initial energies in the direction perpendicular to the magnetic field, the energy gain being of the order of the energy corresponding to the maximum **E**x**B** drift speed, En_{max}, in a like manner to a pickup ion process. It is also found that ions that have initial energies comparable to En_{max} may be decelerated depending upon gyration phase. We find that ions with initial perpendicular energies much larger than En_{max} are little affected along the ion path through KH vortices. By comparing dynamical regimes in the dawn versus and dusk regions, and also by considering different IMF directions, we show that the ion transport across the magnetopause is controlled by the orientation of the magnetosheath electric field and that the rate of energization depends upon the scale of KH vortices versus Larmor radii.

小型磁気圏昼間側マグネトポーズでの電子ダイナミクスに関する全粒子シミュレーション

臼井 英之 [1]; 沖 知起 [2]; 三宅 洋平 [3]; 寺田 直樹 [4]; 関 華奈子 [5]; 八木 学 [6]; 加藤 雄人 [7]
[1] 神戸大・システム情報; [2] 神大・システム・計算; [3] 神戸大学; [4] 東北大・理・地物; [5] 東大理・地球惑星科学専攻; [6] RIKEN R-CCS; [7] 東北大・理・地球物理

Full PIC simulation on the electron dynamics at the dayside magnetopause in a small-scale magnetosphere

Hideyuki Usui[1]; Satoki Oki[2]; Yohei Miyake[3]; Naoki Terada[4]; Kanako Seki[5]; Manabu Yagi[6]; Yuto Katoh[7]
[1] System informatics, Kobe Univ; [2] Kobe Univ.; [3] Kobe Univ.; [4] Dept. Geophys., Grad. Sch. Sci., Tohoku Univ.; [5] Dept. Earth & Planetary Sci., Science, Univ. Tokyo; [6] RIKEN R-CCS; [7] Dept. Geophys., Grad. Sch. Sci., Tohoku Univ.

The objective of this research is to understand the dayside magnetopause physics of a small-scale magnetosphere by performing full particle-in-cell three-dimensional simulations. We define D_p as the distance from the dipole center to the point at which the dynamic pressure of the solar wind and the dipole magnetic pressure are equal. When the ratio ¥lambda$_i$ /D_p is much smaller than the unity where ¥lambda$_i$ denotes the ion inertia length, the formation of the magnetosphere can be examined with the fluid plasma approximation. However, ¥lambda$_i$/D_p becomes close to the unity, the kinetic effect such as finite Lamor radius in plasma cannot be ignored in the formation of the magnetosphere. In the present study, we set ¥lambda$_i$ /D_p =1 to emphasize kinetic effects. When we define R_b as the radius of sphere, we took a relatively large proportion of sphere in the magnetosphere as R_b/D_p=0.6 . In the simulations we found (1) asymmetric structure of the plasma density distribution between the dawn and dusk sides in the magnetic equator, (2) electron acceleration in the magnetic equator at the dayside magnetopause, and (3) plasma perturbation at the dusk side of the plasma pause. In this study, we particularly focus on (2) and (3) stated above and examined them quantitatively by considering the electron trajectories, velocity distributions and the associated local electric fields. We also discuss the dependency of these phenomena on the mass ratio between ion and electron as well as ¥lambda$_i$ /D_p.

本研究では、小惑星や月面磁気異常、水星など、地球よりも十分弱い磁場を持つ天体と太陽風との相互作用により形成される小型磁気圏について、特に赤道面における昼間側マグネトポーズでの電子ダイナミクスに着目する。小型磁気圏物理ではイオン及び電子の運動論効果が重要となるため両方を粒子として扱う全粒子 3 次元シミュレーションを行った。シミュレーション領域中央に弱い磁気ダイポールを持つ小型球体を中央に置き、南向き IMF を持つ太陽風プラズマを境界領域から流し, 小型磁気圏を再現した。小型磁気ダイポール中心から磁気圧と太陽風動圧が釣り合う点までの距離を D_p とすると、D_p が太陽風イオン慣性長 λ_i に対して十分大きい場合は、地球磁気圏のように、太陽風を流体近似した形で磁気圏形成を議論できる。しかし、天体磁場の磁気モーメントが小さくなり D_p が λ_i やイオンラーマ半径などに近づくと磁気圏形成において太陽風プラズマの運動論的効果が無視できなくなる。今回は、運動論的効果を強調させるために λ_i / D_p =1 と設定した。また, 球体半径 R_b を R_b / D_p =0.6 とし、磁気圏における小型天体の割合を比較的大きく取った。これまでのシミュレーション解析により、磁気圏昼間側の特徴的な現象として、(1) 赤道面におけるプラズマ空間分布の dawn-dusk 非対称性, (2) マグネトポーズでの赤道面での電子加速, (3) dusk 側でのプラズマ密度擾乱などが確認された. 今回は特に (2), (3) に着目し, 電子の軌道や速度分布関数と局所電場との関係を定量的に調べるとともに, イオンと電子の質量比や λ_i / D_p への依存性について考察を行った。

月表面から放出される二次イオンの生成過程

加藤 大羽 [1]; 斎藤 義文 [2]; 横田 勝一郎 [3]; 西野 真木 [4]
[1] 東大・理・地惑; [2] 宇宙研; [3] 阪大; [4] 名大 ISEE

Generation process of the secondary ion emitted from lunar surface

Daiba Kato[1]; Yoshifumi Saito[2]; Shoichiro Yokota[3]; Masaki N Nishino[4]
[1] EPS, Univ. of Tokyo; [2] ISAS; [3] Osaka Univ.; [4] ISEE, Nagoya University

Airless bodies without global magnetic fields are directly exposed to the solar wind and micro-meteorites. When the solar photons, neutral and charged particles are incident on a solid surface, the secondary ions are emitted from the bombarded surface. Although the initial energies of such secondary ions are several eV, they are accelerated up to several hundred eV by the solar wind motional electric field and are detected by ion detectors on spacecraft. The secondary ion composition is expected to be used for remote sensing of the solid surface since it depends on the solid surface composition. This remote measurement using the secondary ion complements X-ray fluorescence, gamma-ray spectroscopy and multi-band spectral imaging. However, neither the quantitative observation of the secondary ions nor the detection of the originating points has been made.

In the Moon's case, there are a few major generation mechanisms of the secondary ions; photon-stimulated desorption (PSD) by the solar photons, photoionization of neutral particles, solar wind sputtering and micro-meteoroid impact. The secondary ions generated by PSD consist of Alkali ions such as Na^+ and K^+. In contrast, a variety of ion species can be generated by the ion sputtering and micro-meteoroid impact process. Since the amount of secondary ions depends on the emission mechanisms, analysis of the secondary ion considering generation processes is important.

MAP-PACE-IMA on Kaguya has detected the secondary ions from the Moon. We have investigated a variety of ion species and detected the originating points using the solar wind convection electric field information. We have newly found that there exist ion flux intensity variations that show good correspondence with the location of the lunar magnetic anomalies. This is suggested that the amounts of the secondary ions generated by sputtering are decreased above the lunar magnetic anomalies since the strong magnetic field can prevent the solar wind from impacting the lunar surface. We have estimated the amount of secondary ions generated by the solar wind sputtering by comparing the data obtained above magnetic anomalies and the region without magnetic anomalies. In addition, in order to estimate the influence of the secondary ions generated by micro-meteoroid impact, we have investigated the secondary ion flux when major meteor showers took place.

In conclusion, although the secondary ion observations do not directly reproduce the lunar surface composition, they can be used for remotely sensing the lunar surface composition if we consider the existence of the lunar magnetic anomalies and the generation process of the secondary ions. This measurement is expected to be applied not only to the Moon but also to various astronomical bodies.

全球的な固有磁場も大気も存在しない天体では、太陽風や微小隕石などが天体表面に直接衝突している。このような外部からの中性粒子や荷電粒子、太陽光などが固体表面に入射することで、二次イオンと呼ばれる天体表面起源のイオンが生成される。生成された二次イオンは太陽風の電場によって数 eV から数百 eV にまで加速され、天体上空を周回する探査機で観測することができる。二次イオンの組成は天体表面の元素組成と対応していることから、二次イオン観測による表面構造の遠隔探査が将来可能になることが期待されている。この二次イオンを用いた遠隔測定が確立すれば、X 線分光計やガンマ線分光計などと補完し合いながら天体表面探査が行えるようになる。しかしながら、具体的に二次イオンのイオン種毎の定量的な観測や、観測したイオンの生成地点を特定するといった研究は未だ行われていない。

月の場合、表面からの二次イオン放出メカニズムの主な候補として、太陽光による光脱離や太陽風イオンによるスパッタリング、微小隕石衝突が挙げられる。太陽光による月起源イオンの生成では、Na^+ や K^+ といったアルカリイオンが顕著に放出される。これに対し、太陽風イオンや微小隕石衝突による生成では、月固体表面の組成に応じた様々なイオン種が放出されると考えられている。放出メカニズムによって各種の二次イオン生成量が異なってくるため、二次イオンの生成過程を考慮して分析を行うことが重要である。

月探査衛星「かぐや」に搭載されたイオン観測装置 MAP-PACE-IMA は、月起源の二次イオン観測を行った。本発表では IMA の観測データを用いて、イオン種毎の解析を行い、太陽風電場のベクトルから月表面の生成場所の特定を試みた。二次イオンの生成位置と月表面環境の相関を調べた結果、月表面上の磁気異常領域の分布と相関があることが確認された。これは、月磁気異常による磁気反射によって月面衝突する太陽風が減少するため、スパッタリングによる二次イオンの生成量も減少したためと考えられる。このことから、磁気異常領域と非磁気異常領域での観測データを比較することで、スッパタリング由来の二次イオン生成量を見積もった。また、微小隕石衝突由来の二次イオン生成の度合いを調べるために、流星群が接近した時期の二次イオン生成量に注目した分析を行った。

月起源の二次イオン生成分布と月固体表面の元素組成分布を比較した結果、月周辺の二次イオン観測は月固体表面組成を直接再現はしないが、磁気異常の存在やイオン生成過程の違いを考慮することで、遠隔探査による月表面物質の情報を得ることが可能であることが分かった。この手法は、月以外の天体でも適応可能であるといえる。

Frequency dependence on the beaming angle of Jupiter's decametric radio emissions

Kazumasa Imai[1]; Charles A. Higgins[2]; Masafumi Imai[3]; Tracy Clarke[4]
[1] NIT, Kochi; [2] Middle Tennesee State University; [3] University of Iowa; [4] Naval Research Laboratory

The beaming angle of Jupiter's decametric radio emissions is very important to elucidate the emission mechanism of Jupiter's decametric radio emissions. This beaming angle can be estimated by the modulation lane method [Imai et al., 2017]. The modulation lane method is based on the measurements of the slope of modulation lanes on the dynamic spectrum of Jupiter's decametric radio emissions. We usually measure the slope with a 1 MHz bandwidth and determine the most probable value of the lead angle to fit the value of the slope. The longitudinal location of the magnetic field line of the radio emitting sources can be calculated by the lead angle. Once the location of the source is found, we determine the beaming angle (so-called cone half-angle) as the angle between the direction tangent to the magnetic field line at the source and the direction to the Earth as seen from the source.

The Long Wavelength Array station 1 (LWA1) is a low-frequency radio telescope designed to produce high-sensitivity, high-resolution spectra in the frequency range of 10-88 MHz. The sensitivity of the LWA1, combined with the low radio frequency interference environment, allows us to observe the wide band modulation lanes of Jupiter's decametric radio emissions [Clarke et al., 2014]. We have analyzed the data including the wide band Io-B modulation lanes observed by LWA1. We found a unique event showing curved modulation lanes over a 22 MHz frequency bandwidth from 12 MHz to 34 MHz. By using our modulation lane method we calculated beaming angles of 57 degrees for 12 MHz and 63 degrees for 34 MHz. The difference of the beaming angles is 6 degrees over a 22 MHz frequency range. This means the value of beaming angle is gradually increasing toward the higher emitting frequency. We will discuss this frequency dependence on the beaming angle of Jupiter's decametric radio emissions based on the archived LWA1 data.

References:

Imai, K., C.A. Higgins, M. Imai, and T.E. Clarke, Jupiter's Io-C and Io-B decametric emission source morphology from LWA1 data analysis, in Planetary Radio Emissions VIII, edited by G. Fischer, G. Mann, M. Panchenko, and P. Zarka, Austrian Academy of Sciences Press, Vienna, pp.89-101, 2017.

ひさき衛星の連続監視で明らかにしたイオ火山噴火時のプラズマ質量供給率に対する木星オーロラの応答

木村 智樹 [1]; 平木 康隆 [2]; 垰 千尋 [3]; 土屋 史紀 [4]; 吉岡 和夫 [5]; 村上 豪 [6]; 山崎 敦 [7]; 北 元 [8]; Badman Sarah[6]; 深沢 圭一郎 [9]; 吉川 一朗 [10]; 藤本 正樹 [11]
[1] Tohoku University; [2] 電通大; [3] 情報通信研究機構; [4] 東北大・理・惑星プラズマ大気; [5] 東大・新領域; [6] ISAS/JAXA; [7] JAXA・宇宙研; [8] 東北大・理・惑星プラズマ大気; [9] 京大・メディアセンター; [10] 東大・理・地惑; [11] 宇宙研

Response of Jupiter’s Aurora to Plasma Mass Loading Rate Monitored by the Hisaki Satellite During Volcanic Eruptions at Io

Tomoki Kimura[1]; Yasutaka Hiraki[2]; Chihiro Tao[3]; Fuminori Tsuchiya[4]; Kazuo Yoshioka[5]; Go Murakami[6]; Atsushi Yamazaki[7]; Hajime Kita[8]; Sarah Badman[6]; Keiichiro Fukazawa[9]; Ichiro Yoshikawa[10]; Masaki Fujimoto[11]
[1] Tohoku University; [2] UEC; [3] NICT; [4] Planet. Plasma Atmos. Res. Cent., Tohoku Univ.; [5] The Univ. of Tokyo; [6] ISAS/JAXA; [7] ISAS/JAXA; [8] Tohoku Univ.; [9] ACCMS, Kyoto Univ.; [10] EPS, Univ. of Tokyo; [11] ISAS, JAXA

The production and transport of plasma mass are essential processes in the dynamics of planetary magnetospheres. At Jupiter, it is hypothesized that Io’s volcanic plasma carried out of the plasma torus is transported radially outward in the rotating magnetosphere and is recurrently ejected as plasmoid via tail reconnection. The plasmoid ejection is likely associated with particle energization, radial plasma flow, and transient auroral emissions. However, it has not been demonstrated that plasmoid ejection is sensitive to mass loading because of the lack of simultaneous observations of both processes. We report the response of plasmoid ejection to mass loading during large volcanic eruptions at Io in 2015. Response of the transient aurora to the mass loading rate was investigated based on a combination of Hisaki satellite monitoring and a newly-developed analytic model. We found the transient aurora frequently recurred at a 2-6-day period in response to a mass loading increase from 0.3 to 0.5 ton/s. In general the recurrence of the transient aurora was not significantly correlated with the solar wind although there was an exceptional event with a maximum emission power of 10 TW after the solar wind shock arrival. The recurrence of plasmoid ejection requires the precondition that amount comparable to the total mass of magnetosphere, 1.5 Mton, is accumulated in the magnetosphere. A plasmoid mass of more than 0.1 Mton is necessary in case that the plasmoid ejection is the only process for mass release.

The production and transport of plasma mass are essential processes in the dynamics of planetary magnetospheres. At Jupiter, it is hypothesized that Io ’ s volcanic plasma carried out of the plasma torus is transported radially outward in the rotating magnetosphere and is recurrently ejected as plasmoid via tail reconnection. The plasmoid ejection is likely associated with particle energization, radial plasma flow, and transient auroral emissions. However, it has not been demonstrated that plasmoid ejection is sensitive to mass loading because of the lack of simultaneous observations of both processes. We report the response of plasmoid ejection to mass loading during large volcanic eruptions at Io in 2015. Response of the transient aurora to the mass loading rate was investigated based on a combination of Hisaki satellite monitoring and a newly-developed analytic model. We found the transient aurora frequently recurred at a 2-6-day period in response to a mass loading increase from 0.3 to 0.5 ton/s. In general the recurrence of the transient aurora was not significantly correlated with the solar wind although there was an exceptional event with a maximum emission power of 10 TW after the solar wind shock arrival. The recurrence of plasmoid ejection requires the precondition that amount comparable to the total mass of magnetosphere, 1.5 Mton, is accumulated in the magnetosphere. A plasmoid mass of more than 0.1 Mton is necessary in case that the plasmoid ejection is the only process for mass release.

火山活動活発期における木星衛星イオの酸素原子中性雲の分布

古賀 亮一 [1]; 土屋 史紀 [2]; 鍵谷 将人 [3]; 坂野井 健 [4]; 木村 智樹 [5]; 吉川 一朗 [6]; 吉岡 和夫 [7]; 村上 豪 [8]; 山崎 敦 [9]
[1] 東北大・理・地物; [2] 東北大・理・惑星プラズマ大気; [3] 東北大・理・惑星プラズマ大気研究センター; [4] 東北大・理; [5] Tohoku University; [6] 東大・理・地惑; [7] 東大・新領域; [8] ISAS/JAXA; [9] JAXA・宇宙研

Spatial distribution of Jupiter moon Io’s neutral oxygen cloud during a volcanically active period

Ryoichi Koga[1]; Fuminori Tsuchiya[2]; Masato Kagitani[3]; Takeshi Sakanoi[4]; Tomoki Kimura[5]; Ichiro Yoshikawa[6]; Kazuo Yoshioka[7]; Go Murakami[8]; Atsushi Yamazaki[9]
[1] Geophysics, Tohoku Univ.; [2] Planet. Plasma Atmos. Res. Cent., Tohoku Univ.; [3] PPARC, Tohoku Univ; [4] Grad. School of Science, Tohoku Univ.; [5] Tohoku University; [6] EPS, Univ. of Tokyo; [7] The Univ. of Tokyo; [8] ISAS/JAXA; [9] ISAS/JAXA

A Jupiter’s moon Io is the most volcanically active body in the solar system, and its thin atmosphere is formed by volcanism and sublimation from the surface frost. Neutral particles in the Io’s atmosphere (oxygen and sulfur atoms, and their components) escape from Io’s gravity mainly by atmospheric sputtering, and form neutral clouds around Io’s orbit. The previous modeling studies showed the equilibrium spatial distibution of the neutral oxygen and sulfur clouds. The relationship between infrared emissions of Io’s volcanoes and sodium nebula emissions by ground-based observations showed that the amount of neutrals escaped from Io increases during major volcanic eruptions. If the spatial distribution of the neutal clouds during a volcanically active period is found, other parameters such as profile of exosphere, speed distribution and direction are constrained, and it is understood how the change in the volcanic activity of Io affects the escape process of neutrals. In this study, we aim to understand the spatail distribution of Io’s neutral oxygen cloud by using the ultraviolet spectral data obtained with the Hisaki satellite.

Atomic oxygen emission at 130.4 nm aroud Io’s orbit was weak from November to December in 2014, but it was intense from January to April in 2015 (the brightness was 2-2.5 times as large as usual). de Kleer and de Pater [2016] reported the enhancement of infrared emissions at Mithra Patera in 10 January 2015, and at Kurdalagon Patera in 26 January and 5 April 2015. These volcanoes may increase the source of the neutral clouds. Using the data taken by Hisaki, we analyzed the Io phase angle dependece of atomic oxygen emission during volcanically quiet (from November to December in 2014) and active periods (from January to April in 2015). The azimuthal distribution duirng the volcanically quiet period shows Io’s neutral oxygen cloud consists of two components, a cloud concentrated around Io that spreads leading and Jupiterword direction (called ””banana cloud””) and a longitudinally uniform, diffuse distribution along Io’s orbit. However, the distirbution of the banana cloud changed from March to April in 2015. The banana cloud spreads mainly in the trailing and anti Jupiterward direction, or spreads in the both leading and trailing direction. The speed distribution and direction in the case that only oxygen atoms collide with torus ions is different from those in the case that SO_2 collide with torus ions and then oxygen atoms are escaped. A possible explaniation is that variations of the profile of Io’s exosphere or the plasma temperature around Io may change the ratio of SO_2 and O which collide with torus ions, and then change the shape of the banana cloud.

Azimuthal variation in the Io plasma torus observed by the Hisaki satellite from 2013 to 2016

Fuminori Tsuchiya[1]; Ryo Arakawa[2]; Hiroaki Misawa[3]; Masato Kagitani[4]; Ryoichi Koga[5]; Fumiharu Suzuki[6]; Reina Hikida[7]; Kazuo Yoshioka[8]; Tomoki Kimura[9]; Yasumasa Kasaba[10]; Go Murakami[11]; Ichiro Yoshikawa[12]; Atsushi Yamazaki[13]

[1] Planet. Plasma Atmos. Res. Cent., Tohoku Univ.; [2] Geophysics, Tohoku Univ.; [3] PPARC, Tohoku Univ.; [4] PPARC, Tohoku Univ; [5] Geophysics, Tohoku Univ.; [6] Complexity Science, Univ. of Tokyo; [7] Frontier Sciences, Tokyo Univ.; [8] The Univ. of Tokyo; [9] Tohoku University; [10] Tohoku Univ.; [11] ISAS/JAXA; [12] EPS, Univ. of Tokyo; [13] ISAS/JAXA

http://pparc.gp.tohoku.ac.jp/

The inner area of a planetary magnetosphere generally contains a dense plasma region that corotates with the planet. In the Jovian magnetosphere, sulfur and oxygen ions supplied by the satellite Io are distributed in what is called the Io plasma torus. Various plasma parameters in the plasma torus have significant azimuthal variations that are coupled with the energy flows in the Jovian inner magnetosphere. In this study, 3 years of data obtained by the Hisaki satellite, from December 2013 to August 2016, were used to investigate statistically the azimuthal variations and to find how the variations were influenced by productions of plasma from Io. The azimuthal variation was obtained from a time series of sulfur ion line ratios, S^{3+} 65.7 nm/S^{3+} 140.5 nm and S^{3+} 65.7 nm/S^{+} 76.5 nm, which were sensitive to the electron temperature and the sulfur ion mixing ratio S^{3+}/S^{+}, respectively. Using the two line ratios, we confirmed significant single peaked azimuthal variations in the thermal electron temperature and the S^{3+}/S^{+} mixing ratio in the Io plasma torus. The mean rotation rate of the azimuthal patterns during the 3 years of Hisaki observations was found to be 10.08 h, 1.5% slower than the Jovian rotation period. The azimuthal variation of the S^{3+}/S^{+} mixing ratio is nearly in phase with that of the thermal electron temperature. The peak longitude of the electron temperature tends to precede that of the higher sulfur ion charge state (S^{3+}/S^{+}) by 0 deg-90 deg, which is explained by the competing effect of the sub-corotation of hot electrons and chemical reactions in the plasma torus. These results are consistent with the prediction of the dual hot electron model proposed to explain previous observations (Steffl et al., 2008; Hess et al., 2011). One of new findings from the Hisaki observation is change in the rotation period of the plasma torus associated with Io volcanic activity. The rotation period sometimes decreased from the mean periodicity of 10.08 h. The period fell to 9.93-9.97 h in March April 2015 and to 10.03 h in May June 2016. The decreases in the rotation period in 2015 and 2016 were related to the increase in Io volcanic activity. Both decreases occurred when the thermal electron temperature in the plasma torus increased. On the other hand, the decrease in the rotation period occurred in February 2014 when there was no increase in Io's volcanic activity and no observed increase in the thermal electron temperature. Hisaki also found that a double-peaked azimuthal compoment in the S^{3+}/S^{+} ratio and thermal electron temperature. The S^{3+}/S^{+} ratio was located not only around 0 deg-45 deg, as in previous observations, but also around ˜180 deg. The origin of the double-peaked structure is an open question and further study is needed to resolve it.

イオプラズマトーラスのエネルギー収支

吉川 一朗 [1]; ひさき（SPRINT-A）プロジェクトチーム 山崎　敦 [2]
[1] 東大・理・地惑; [2] -

Energy budget in the IPT system: How does the IPT radiate intensively in the UV-EUV spectral region?

Ichiro Yoshikawa[1]; Yamazaki Atsushi Hisaki (SPRINT-A) project team[2]
[1] EPS, Univ. of Tokyo; [2] -

One of the focal points of interest in the IPT system is the transport of energy and particles into the inner region. Delamere and Bagenal (2011) estimated the total energy budget of the IPT system, suggesting that hot electrons must be added to the system (See Figure 9 in their paper). Their estimate stated that UV radiation would reduce by 30-70% without the hot electrons in the system. To explain present brightness of the IPT, the IPT must be fueled up by 30-70%. Therefore, they explicitly assumed the existence of hot electrons in their calculation and found reasonable solutions regarding energy and mass budges in the IPT system, but this assumption has not been justified yet. Recently, we have taken the advantage of long-term and quasi-continuous simultaneous monitoring of the polar aurora and the Io Plasma Torus (IPT) located in the inner magnetosphere by Extreme Ultraviolet Spectroscope for Exospheric Dynamics/Hisaki. Studies on temporal characteristics over hours enabled us to see slow (˜10 h) coupling between the middle and inner magnetosphere as well as to quantify the temperature of hot electrons in the IPT. Furthermore, volcanic eruption in 2015 gave us opportunity to see how the IPT reacted to this event and how much energy was added to the system. We will discuss this classical issue, so-called Energy Crisis, by using Hisaki EUV spectrum.

MAVENの火星磁気リコネクション観測

原田 裕己 [1]; Halekas Jasper S.[2]; DiBraccio Gina[3]; Xu Shaosui[4]; Espley Jared R.[3]; McFadden James P.[5]; Mitchell David L.[5]; Mazelle Christian[6]; Brain David A.[7]; 原 拓也 [5]; Ma Yingjuan[8]; Ruhunusiri Suranga[9]; Jakosky Bruce M.[10]
[1] 京大・理・地球惑星; [2] Dept. Phys. & Astron., Univ. Iowa; [3] NASA GSFC; [4] SSL, UCB; [5] SSL, UC Berkeley; [6] CNRS,IRAP; [7] LASP, Univ. of Colorado at Boulder, USA; [8] UCLA; [9] Univ. of Iowa; [10] LASP, CU Boulder

MAVEN observations of magnetic reconnection signatures at Mars

Yuki Harada[1]; Jasper S. Halekas[2]; Gina DiBraccio[3]; Shaosui Xu[4]; Jared R. Espley[3]; James P. McFadden[5]; David L. Mitchell[5]; Christian Mazelle[6]; David A. Brain[7]; Takuya Hara[5]; Yingjuan Ma[8]; Suranga Ruhunusiri[9]; Bruce M. Jakosky[10]
[1] Dept. of Geophys., Kyoto Univ.; [2] Dept. Phys. & Astron., Univ. Iowa; [3] NASA GSFC; [4] SSL, UCB; [5] SSL, UC Berkeley; [6] CNRS,IRAP; [7] LASP, Univ. of Colorado at Boulder, USA; [8] UCLA; [9] Univ. of Iowa; [10] LASP, CU Boulder

http://www-step.kugi.kyoto-u.ac.jp/members/staff/haraday.html

It has been speculated that magnetic reconnection could occur frequently in the near-Mars space, given the complex magnetic field configuration resulting from interaction between crustal and interplanetary magnetic fields. However, definitive identification of in-situ reconnection signatures has been elusive due to the lack of comprehensive particle and field instrumentation on the past Mars missions. Here we investigate the occurrence and characteristics of magnetic reconnection in the Martian magnetosphere by utilizing ion, electron, and magnetic field measurements by the Mars Atmosphere and Volatile EvolutioN (MAVEN) mission. We identified current sheet crossing events with a collection of reconnection signatures including (i) Alfvenic ion flows within current sheets, (ii) Hall magnetic fields, (iii) nonzero normal fields, and (iv) closed field topology on both the dayside and the nightside of Mars. Many reconnection events observed by MAVEN exhibit mass-dependent ion flows, highlighting two important aspects of the plasma environment of Mars: (i) the presence of heavy ions (predominantly atomic and molecular oxygen ions) along with protons and (ii) the smallness of the system size with respect to the ion scale length. Statistical investigation of Hall magnetic fields and accelerated ion flows in nightside magnetotail current sheets suggests that magnetic reconnection operates for at least ~1-10% of the time in tail current sheets. Furthermore, analysis of magnetic topology inferred from electron energy and pitch angle distributions revealed that the coexistence of trapped electrons of solar wind and ionospheric origins on the same closed field line, which is indicative of recent closure of open field lines by reconnection, is observed relatively frequently with ~1-10% occurrence rates in the nightside magnetosphere. Taken together, these MAVEN observations demonstrate that magnetic reconnection is not uncommon in the near-Mars space. This result has important implications for the formation and dynamics of the Martian magnetosphere such as the twisted magnetotail configuration, formation of magnetic flux ropes, and electron injection on closed crustal field lines.

MAVEN観測に基づく火星磁気圏尾部からの重イオン流出に関する統計的研究

乾 彰悟 [1]; 関 華奈子 [2]; 堺 正太朗 [2]; Brain David A.[3]; 原 拓也 [4]; McFadden James P.[4]; Halekas Jasper S.[5]; Mitchell David L.[4]; DiBraccio Gina[6]; Jakosky Bruce M.[7]
[1] 東大・理・地惑; [2] 東大理・地球惑星科学専攻; [3] LASP, Univ. of Colorado at Boulder, USA; [4] SSL, UC Berkeley; [5] Dept. Phys. & Astron., Univ. Iowa; [6] NASA GSFC; [7] LASP, CU Boulder

Statistical study of heavy ion outflows from Mars observed in the Martian induced magnetotail by MAVEN

Shogo Inui[1]; Kanako Seki[2]; Shotaro Sakai[2]; David A. Brain[3]; Takuya Hara[4]; James P. McFadden[4]; Jasper S. Halekas[5]; David L. Mitchell[4]; Gina DiBraccio[6]; Bruce M. Jakosky[7]
[1] Earth and Planetary Science, Univ. of Tokyo; [2] Dept. Earth & Planetary Sci., Science, Univ. Tokyo; [3] LASP, Univ. of Colorado at Boulder, USA; [4] SSL, UC Berkeley; [5] Dept. Phys. & Astron., Univ. Iowa; [6] NASA GSFC; [7] LASP, CU Boulder

Mars does not have a global intrinsic magnetic field. Therefore, planetary ion escape through interaction between the solar wind and the Martian upper atmosphere is one of the candidate mechanisms of the atmospheric escape. On the other hand, Mars has local crustal magnetic fields. Effects of these crustal magnetic fields on atmospheric escape are far from understood. In this study, we report on a statistical analysis of heavy ion outflows from Mars in order to understand influences of the local crustal magnetic fields and the direction of solar wind electric field on the ion outflows based on the MAVEN satellite observations. Data from the STATIC (ion composition), SWIA (solar wind ion), and MAG (magnetic field) instruments from Nov. 2014 to Dec. 2017 were used for the statistical study. We focused on the heavy ion outflows in the magnetotail wake region.

Based on the analysis method used in the previous study [Inui et al., GRL, 2018], we investigated properties of O+, O2+, and CO2+, separately. We divided data by the location of the strong local crustal magnetic field around east longitude of 180 degrees into 4 local time groups: noon, dawn, dusk, and night. We also divided the data by locations of the ion outflow detection: upward E and downward E hemispheres in the Mars-Solar-Electric field (MSE) coordinates and north and south hemispheres in the Mars-Solar-Orbital (MSO) coordinates. The results show that number densities of heavy ions observed in the downward E hemisphere in the MSE coordinates tend to be higher than those observed in the upward E hemisphere, while the trend of heavy ion bulk velocity is opposite. The results also show that the number fluxes of escaping heavy ions are larger in downward E hemisphere than in upward E hemisphere. However, we do not find the clear evidence that the location of the strong crustal magnetic field affects the statistical properties of the heavy ion outflows. We also report on the ratio of the three ion species in the outflows.

太古の火星からのイオン散逸に対する弱い固有磁場の影響

坂田 遼弥 [1]; 関 華奈子 [1]; 堺 正太朗 [1]; 寺田 直樹 [2]; 品川 裕之 [3]; 田中 高史 [4]
[1] 東大理・地球惑星科学専攻; [2] 東北大・理・地物; [3] 情報通信研究機構; [4] 九大・国際宇宙天気科学教育センター

Effects of a weak planetary intrinsic magnetic field on the ion loss from ancient Mars

Ryoya Sakata[1]; Kanako Seki[1]; Shotaro Sakai[1]; Naoki Terada[2]; Hiroyuki Shinagawa[3]; Takashi Tanaka[4]
[1] Dept. Earth & Planetary Sci., Science, Univ. Tokyo; [2] Dept. Geophys., Grad. Sch. Sci., Tohoku Univ.; [3] NICT; [4] REPPU code Institute

Mars had a thick atmosphere and liquid water in ancient days but lost most of them. One of the candidate processes of the removal of the atmosphere is the ion loss. The ancient solar XUV (X-ray and extreme ultra-violet) irradiance was more intense and the ancient solar wind was faster and denser. Recent studies have pointed out that the ion loss rate at Mars increases several orders of magnitude under such severer solar conditions. On the other hand, the existence of the crustal magnetic field suggests that ancient Mars had an intrinsic magnetic field. The existence of an intrinsic magnetic field can affect the structure of the magnetosphere and thus the ion loss processes. To understand the atmospheric escape from ancient Mars, it is important to investigate how the intrinsic magnetic field influences the ion loss processes.

We studied the ion loss processes from early Mars under ancient solar conditions and the existence of weak intrinsic magnetic field with magnetohydrodynamic (MHD) simulations. We used 3D multi-species MHD model introduced by Terada et al. (2009a) and added the planetary intrinsic magnetic field. We assumed that the interplanetary magnetic field was a parker spiral and solar wind proton density, the solar wind velocity, and the solar XUV flux were 1000 /cm^3, 2000 km/s, and 100 times higher than the present-day XUV flux, respectively. These parameters are same as those used in Terada et al. (2009b), in which the neutral atmosphere profile of ancient Mars is adopted from the model introduced by Kulikov et al. (2007). We conducted three cases of simulations with different intrinsic magnetic field conditions, that is, dipole fields with the strength of 0 nT, 100 nT, and 1000 nT on the equatorial surface. It should be noted that the dynamic pressure of the solar wind in this study is equivalent to the magnetic pressure of field strength of 4100 nT.

The results of 1000 nT case show that the tailward flux structure and the plasma sheet in the tail region incline towards the dusk side in the northern hemisphere and towards the dawn side in the southern hemisphere. Also, the escape rates of heavier ions such as CO_2^+ and O_2^+ are several times higher than those with no (0 nT) intrinsic magnetic field. The escape channels of these ions correspond to the open magnetic field lines, that is, the field lines with one end connected to the planet and the other end connected to the interplanetary magnetic field. These phenomena are due to the magnetic reconnection between the intrinsic magnetic field and the interplanetary magnetic field. The increases in escape rates of heavy ions and the reconnections in the tail region also occur in 100 nT case. However, the inclination of the tailward-flux structure and the correspondence of the escape channels to the open field lines are less distinct. The structure of tailward flux is along to the plasma sheet with no (0 nT) intrinsic magnetic field.

References:

Kulikov, Y. N., Lammer, H., Lichtenegger, H. I. M., et al. (2007). A comparative study of the influence of the active young sun on the early atmospheres of Earth, Venus, and Mars. *Space Science Reviews, 129*(1-3), 207-243. https://doi.org/10.1007/s11214-007-9192-4

Terada, N., Kulikov, Y. N., Lammer, H., Lichtenegger, H. I. M., Tanaka, T., Shinagawa, H., & Zhang, T. (2009b). Atmosphere and Water Loss from Early Mars Under Extreme Solar Wind and Extreme Ultraviolet Conditions. *Astrobiology, 9*(1), 55-70. https://doi.org/10.1089/ast.2008.0250

Terada, N., Shinagawa, H., Tanaka, T., Murawski, K., & Terada, K. (2009a). A three-dimensional, multispecies, comprehensive MHD model of the solar wind interaction with the planet Venus. *Journal of Geophysical Research: Space Physics, 114*(9), 1-11. https://doi.org/10.1029/2008JA013937

超小型探査機による大気・プラズマの光学観測

吉岡 和夫 [1]; 桑原 正輝 [2]; 疋田 伶奈 [3]; 田口 真 [4]; 川原 琢也 [5]; 亀田 真吾 [6]; 吉川 一朗 [7]
[1] 東大・新領域; [2] 東大・新領域・複雑理工; [3] 東大・新領域・複雑理工; [4] 立教大・理・物理; [5] 信州大・工; [6] 立教大; [7] 東大・理・地惑

The remote observation for space plasma and atmosphere using the ultra-small spacecraft

Kazuo Yoshioka[1]; Masaki Kuwabara[2]; Reina Hikida[3]; Makoto Taguchi[4]; Takuya Kawahara[5]; Shingo Kameda[6]; Ichiro Yoshikawa[7]
[1] The Univ. of Tokyo; [2] The Univ. of Tokyo; [3] Frontier Sciences, Tokyo Univ.; [4] Rikkyo Univ.; [5] Faculty of Engineering, Shinshu University; [6] Rikkyo Univ.; [7] EPS, Univ. of Tokyo

The missions for planetary science using ultra-small spacecraft which is less than 100 kg are developed at various universities and research institutes in Japan and other countries. Remote observation using the emissions from the target bodies and atmospheres is a very important and powerful tool in such a plan that is required for quickness and flexibility because of severe constraints on budget and time. In this presentation, the specification and development status of the optical instrument mounted on the ultra-small spacecraft (EQUULEUS) which will be launched in 2019 is introduced. The principle of a method for measuring the isotopic compositions of planetary bodies such as "D/H absorption-cell method" will also be shown.

2014年にはやぶさ２探査機の相乗りとして打ち上げられたＰＲＯＣＹＯＮを始めとして、超小型探査機による太陽系天体の観測計画が、国内外の大学・研究機関で進められている。予算や開発期間に厳しい制約があるため即応性と柔軟性が要求されるこの様な計画において、光を用いた遠隔観測は重要かつ強力な手段である。本発表では、2019年の打上を目指して開発が進められている超小型探査機（EQUULEUS）に搭載される光学観測装置（PHOENIX）の開発状況を紹介する。さらに、超小型の特性を活かした観測技術の代表として、吸収セルを用いた分光観測について、試作機の開発現状とその応用可能性について議論する。

Low electron temperatures observed at Mars by MAVEN on dayside crustal magnetic field lines

Shotaro Sakai[1]; Thomas E. Cravens[2]; Laila Andersson[3]; Christopher M. Fowler[3]; David L. Mitchell[4]; Christian Mazelle[5]; David A. Brain[6]; Edward M. B. Thiemann[3]; Francis G. Eparvier[3]; Kanako Seki[1]
[1] Dept. Earth & Planetary Sci., Science, Univ. Tokyo; [2] U. Kansas; [3] LASP, CU Boulder; [4] SSL, UC Berkeley; [5] CNRS,IRAP; [6] LASP, Univ. of Colorado at Boulder, USA

The current Mars only has a thin atmosphere and little water on the surface, whereas Mars had a thick atmosphere in the past. This suggests that Mars has experienced significant atmospheric loss. The ionospheric electron temperature is particularly important for determining the neutral/photochemical escape rate from the Martian atmosphere. The Langmuir Probe and Waves instrument onboard MAVEN (Mars Atmosphere and Volatile EvolutioN) measures electron temperatures in the ionosphere of Mars. The current paper studies temperatures in the dayside for two regions where: (1) crustal magnetic fields are dominant and (2) draped magnetic fields are dominant. On average, the electron temperature is lower in the crustal-field regions, which we suggest is due to a closer connection along magnetic field lines between cold electrons at lower altitudes, where the neutral density and associated cooling rates are greatest, and the upper atmosphere. Electron heat conduction in the crustal-field regions could be altered due to the magnetic mirror force and/or the ambipolar electric field above 250 km altitude. Both effects should be considered for future simulation studies.

Seasonal variation of the homopause altitudes on Mars derived from MAVEN/IUVS observations

Nao Yoshida[1]; Hiromu Nakagawa[2]; Naoki Terada[3]; Hitoshi Fujiwara[4]; Takeshi Imamura[5]
[1] Geophysics, Tohoku Univ.; [2] Geophysics, Tohoku Univ.; [3] Dept. Geophys., Grad. Sch. Sci., Tohoku Univ.; [4] Faculty of Science and Technology, Seikei University; [5] The University of Tokyo

The altitude of the homopause can be controlled by the solar flux, global circulation and gravity wave breaking. The atmosphere below the homopause is well mixed by the eddy diffusion. Above the homopause, the mixing ratios of lighter species increase with height due to the molecular-diffusion separation. Therefore, the homopause altitude is a key to understanding the atmospheric constituents at exobase that has been lost to space. In addition, the turbopause, which is located at almost the same altitude as the homopause, is defined as the altitude where the molecular diffusion coefficient is equal to the eddy diffusion coefficient. The former coefficient can be derived from a number density. Although the eddy diffusion coefficient is hard to constrain by observations and had large uncertainties, it can be constrained by the homopause altitude.

On Mars, there have been a few limited observations of the homopause so far. The Viking probe was the first to suggest that it was located at ˜120-130 km altitude. Recently, Jakosky et al. [2017] showed substantial variation of the homopause altitude from February 2015 to June 2016 using data from in-situ measurements onboard MAVEN spacecraft. Due to the limitation of orbital motion of MAVEN, the main controlling factor of the variations has yet to be fully characterized. This measurement is usually made above ˜150 km altitude, which cannot reach the homopause, therefore they have to assume isothermal temperature atmosphere to infer the homopause altitude.

We aim to investigate the dayside homopause altitude on Mars using N_2/CO_2 density profiles derived from remote-sensing measurements by Imaging Ultraviolet Spectrograph (IUVS) onboard MAVEN. IUVS limb mode can retrieve N_2 and CO_2 density profiles from 130 to 220 km altitude, which covers the altitude range between the homopause and upper thermosphere. Both scale heights of N_2 and CO_2 density profiles below ˜150 km altitude have a similar trend. In contrast, they show different scale heights above ˜150 km altitude due to the diffusive separation. These profiles well represent the transition region between the well-mixed lower atmosphere, and the diffusive upper atmosphere. This feature implies that IUVS limb observations clearly captured the homopause.

Here, in order to estimate the homopause altitude from N_2/CO_2 profile, we applied a third polynomial fit between 130 and 193 km altitude range for averaged N_2/CO_2 for each orbit. The inferred homopause altitudes significantly change along time with a large-scale sinusoidal trend. The higher homopause (160-170 km) appears during the perihelion. The lower homopause (130-150 km) appears during the aphelion. We concluded that the dayside homopause altitudes are mainly driven by changing solar forcing due to heliocentric distance over longer time-scale. Furthermore, the inferred homopause altitudes gradually decrease throughout the mission with by ˜5 km from Martian Year (MY) 32 to MY33, which seems to be caused by the decrease in solar EUV. Our result represents a complicated combination of lower and upper atmospheric forcing upon the homopause altitude.

We have also characterized N_2/CO_2 profiles for each season. These data suggest that N_2/CO_2 profiles can be classified by depending on the season. Resulting N_2 to CO_2 mixing ratio at ˜190 km altitude in northern winter could have more than one-order larger than in northern summer. These differences are partly influenced by the homopause altitudes. Our result indicates the significant difference of atmospheric composition to be escaped in season.

We discussed the eddy diffusion coefficient at the homopause using our result. The eddy diffusion coefficient at the homopause is in the order of ˜10^4. This value is comparable order to that derived from the Viking probes. Our result shows no clear seasonal variation but gradually decreases throughout the mission.

Exploring the Atmosphere of Mars with Remote Observations and Numerical Studies: Belgium-Japan partnership 2017-2019

Yasumasa Kasaba[1]; Hiromu Nakagawa[2]; Hideo Sagawa[3]; Takeshi Kuroda[4]; Takeshi Imamura[5]; Ann Carine VANDAELE[6]; Shohei Aoki[7]; Isao Murata[8]; Naoki Terada[9]; Takeshi Sakanoi[10]; Yasuko Kasai[4]; Atsushi Yamazaki[11]; Takao M. Sato[12]; Hiroyuki Maezawa[13]; Hiroki Kashimura[14]; Makoto Taguchi[15]; Severine ROBERT[6]; Valerie WILQUET[6]; Arnaud MAHIEUX[6]; Kosuke Takami[2]; Sae Aizawa[16]; Masashi Toyooka[2]; Takehiko Akiba[17]; Nao Yoshida[18]

[1] Tohoku Univ.; [2] Geophysics, Tohoku Univ.; [3] Kyoto Sangyo University; [4] NICT; [5] The University of Tokyo; [6] BISA; [7] BIRA-IASB; [8] Environmental Studies, Tohoku Univ.; [9] Dept. Geophys., Grad. Sch. Sci., Tohoku Univ.; [10] Grad. School of Science, Tohoku Univ.; [11] ISAS/JAXA; [12] ISAS/JAXA; [13] none; [14] Planetology/CPS, Kobe Univ.; [15] Rikkyo Univ.; [16] Geophysics, Tohoku Univ; [17] Geophysics,Tohoku Univ.; [18] Geophysics, Tohoku Univ.

Recent successful explorations of Mars and Venus atmospheres by numerous spacecraft and ground-based telescopes have suggested their active photochemistry and dynamics. Characteristics of spatial and temporal variations of temperature, wind, and atmospheric constituents are essential to understand the photochemistry and dynamics. From April 2017 to March 2019, Japan-Belgium collaboration program, AMAVERO (Exploring the Atmosphere of MArs and VEnus with Remote Observations: A Belgium-Japan partnership) is running. In this project, we study the following aspects. (1) 3D distributions (i.e., spatial variation + vertical profiles) of temperature, wind, and trace gases on Mars, and (2) those at the middle atmosphere (from the cloud top to the upper atmosphere, 60-140 km) of Venus.

These objectives are achieved by collecting observational datasets from Belgium and Japan. Belgian side provides the data taken by European Mars orbiter Mars Express (MEx) and Trace Gas Orbiter (TGO), and Venus Orbiter Venus Express (VEx). From Japan, we provide the data taken by ground-based and spaceborne telescopes with Japanese Venus Orbiter Akatsuki. Moreover, we share tools to analyze the observational datasets, and develop the numerical models of the atmospheres to interpret the observational results. We are executing the following researches based on the exchange of young research staffs, postdocs, and graduate school students: (1) Collaboration of ground-based observations by ALMA sub-mm array, SOFIA IR airborne telescope, and MIRAHI IR heterodyne spectrometer. (for Mars + Venus). (2) Development of Limb retrieval code JACOSPAR for the utilization to ExoMars Trace Gas Orbiter and its test application for H2O vertical profile derived from Mars Express data. (for Mars: to be appeared in this meeting as Toyooka et al.). (3) Distribution and dynamics of Venusian atmosphere observed by Akatsuki IR imagers. (Venus). (4) The inter-comparison of Venusian and Martian GCMs with cloud and water cycles in different approaches. (for Mars + Venus) (5) Variation of the homopause and atmospheric composition in the upper atmosphere with the comparison between VEX/SOIR + MAVEN + TGO with numerical simulations.

This project was generated from the long-term collaborations between Japan and European groups for Mars and Venus sciences associated with Mars Express (2003-), Venus Express (2005-2015), CrossDrive project (Collaborative Virtual Environments for Mars Science Analysis and Rover Target Planning, 2014-2016), ExoMars TGO (2016-), with groundbased and numerical simulation works. In this meeting, we show the progress and the activities on-going in this project related to Mars Express and ExoMars with the link to MAVEN. In 2018, hot studies are now executed for the Martial global dust storm occurred in summer. Now, we try to extend this project with additional two years in order to cover the full TGO observational activities linked to (1)-(5). Those activities will be extracted to the collaboration of future missions in Japan (e.g. MMX) and Europe (e.g. M4 Venus mission study). Any proposals and collaborations are welcomed

ひさき・あかつき同時観測による金星雲層・熱圏上下結合の研究

奈良 佑亮 [1]; 今村 剛 [2]; 吉川 一朗 [3]; 吉岡 和夫 [4]; 益永 圭 [5]; 山崎 敦 [6]; 渡部 重十 [7]; 山田 学 [8]; Lee Yeon Joo[9]; 寺田 直樹 [10]; 関 華奈子 [11]
[1] 東大・新領域; [2] 東京大学; [3] 東大・理・地惑; [4] 東大・新領域; [5] 東大・理
; [6] JAXA・宇宙研; [7] 北大・理・宇宙; [8] 千葉工大・惑星探査研究センター; [9] JAXA/ISAS; [10] 東北大・理・地物; [11] 東大理・地球惑星科学専攻

Interaction between the thermosphere and the cloud-level atmosphere of Venus studied with observations by Hisaki and Akatsuki

Yusuke Nara[1]; Takeshi Imamura[2]; Ichiro Yoshikawa[3]; Kazuo Yoshioka[4]; Kei Masunaga[5]; Atsushi Yamazaki[6]; Shigeto Watanabe[7]; Manabu Yamada[8]; Yeon Joo Lee[9]; Naoki Terada[10]; Kanako Seki[11]
[1] GSFS, Univ. Tokyo; [2] The University of Tokyo; [3] EPS, Univ. of Tokyo; [4] The Univ. of Tokyo; [5] Univ. Tokyo; [6] ISAS/JAXA; [7] Cosmosciences, Hokkaido Univ.; [8] PERC/Chitech; [9] JAXA/ISAS; [10] Dept. Geophys., Grad. Sch. Sci., Tohoku Univ.; [11] Dept. Earth & Planetary Sci., Science, Univ. Tokyo

Observations of the Venus' upper atmosphere using the Extreme Ultraviolet Spectroscope for Exospheric Dynamics (EXCEED) on the space telescope Hisaki revealed the existence of periodical variations in airglow intensities on the dawn side, suggesting that atmospheric waves propagate from the lower atmosphere up to the thermosphere to cause oxygen density variations (e.g., Masunaga et al., 2017). To confirm such vertical coupling via propagating waves, simultaneous observations of the cloud-level atmosphere (~50 –70 km altitude) and the thermosphere are required.

Spacecraft Akatsuki has been orbiting Venus since December 2015 and is observing the cloud-level atmosphere. In June 2017, Hisaki and Akatsuki observed Venus upper and middle atmosphere, respectively. We analyzed time series of the EUV OI (130.4 nm and 135.6 nm) dayglow intensity measured by EXCEED and the UV brightness (365 nm) obtained by the Ultraviolet Imager (UVI) on board Akatsuki. The OI intensity reflects the column densities of oxygen atoms and photoelectrons in the thermosphere, and the UVI images present dark and bright contrasts of clouds, allowing wind retrieval from cloud tracking.

In both data, we identified the same periodicity of 3.5 days. As UVI's 3.5-day periodicity seems to be associated with Kelvin waves at the cloud top, we calculated damping time and amplitudes of the Kelvin waves propagating vertically in a simple model. The model calculation shows that Kelvin waves should decay with height through radiative damping and will not reach the thermosphere. Therefore, we propose an indirect process in which the Kelvin waves change the wind field periodically and this oscillating wind influences the vertical propagation of small-scale gravity waves as discussed in Masunaga et al. (2017). The gravity waves that reach the thermosphere would cause the variation of the diffusion coefficient or the large-scale circulation. We discuss the effect of the variation of the diffusion coefficient on the OI column density using a photochemical model.

回転不変位相相関限定法を用いた金星極域の雲追跡

武藤 圭史朗 [1]; 今村 剛 [2]; 渡部 重十 [3]; 山田 学 [4]; 山崎 敦 [5]
[1] 東大・新領域・複雑理工; [2] 東京大学; [3] 北大・理・宇宙; [4] 千葉工大・惑星探査研究センター; [5] JAXA・宇宙研

Cloud tracking in the Venusian polar region using Rotation Invariant Phase Only Correlation

Keishiro Muto[1]; Takeshi Imamura[2]; Shigeto Watanabe[3]; Manabu Yamada[4]; Atsushi Yamazaki[5]
[1] Complexity Science and Engineering, The Univ. of Tokyo; [2] The University of Tokyo; [3] Cosmosciences, Hokkaido Univ.; [4] PERC/Chitech; [5] ISAS/JAXA

The atmospheric circulation and the associated material transport in the Venusian polar region are thought to be crucial for the maintenance of the global cloud/atmospheric structure. In the ultraviolet range, Venusian cloud shows various patterns created by the transport of ””unknown”” UV absorber, which can provide information both on dynamics and chemistry in this region. Wind velocities have been measured by cloud tracking using images obtained sequentially in such ultraviolet range with Galileo, Venus Express and Akatsuki, using polar projections to avoid the geometrical distortion that high-latitude features present when using equirectangular projections. However, tracking cloud patterns on polar projections presents an additional difficulty due to the need of accounting for the changes in the orientation of the cloud patterns experiencing zonal displacements. In this study, we apply cloud tracking to the polar region in polar projections by using the ””rotation invariant phase only correlation method”” considering the rotation of the cloud patterns. The derived velocity field is compared with the cloud morphology to understand the role of dynamics in shaping the clouds. The data used are 365 nm images taken by UVI onboard JAXA’ Akatsuki. We also derive rotational components from the rotation angle of the image and examine the difference between rotational component obtained from the wind field and obtained from the rotation angle of the image.

あかつき搭載LIRを用いた金星雲頂の温度変動の周期解析

梶原 直也 [1]; 今村 剛 [1]; 田口 真 [2]; 福原 哲哉 [3]; 神山 徹 [4]
[1] 東京大学; [2] 立教大・理・物理; [3] 立教大・理; [4] 産総研

Periodic analysis of Venus' cloud-top temperature fluctuation using by LIR images

Naoya Kajiwara[1]; Takeshi Imamura[1]; Makoto Taguchi[2]; Tetsuya Fukuhara[3]; Toru Kouyama[4]
[1] The University of Tokyo; [2] Rikkyo Univ.; [3] Rikkyo Univ.; [4] AIST

The mechanism of Venus' strong zonal wind blowing at 60 times the speed of its rotation, called the super-rotation, is still unclear. Various waves of planetary scale have been proposed as the cause of the super-rotation, but it has not been elucidated yet.

Planetary-scale waves are known to exist in the atmosphere of Venus. For example, periodic fluctuations with periods of 4 to 5 days in UV brightness were discovered at the cloud top by Pioneer Venus orbiter (DelGenio and Rossow1990). Analyses of velocity fields obtained by cloud tracking revealed that zonal and meridional winds also fluctuate with periods of 4 to 5 days (Rossow et al. 1990; Kouyama et al. 2012, 2015). It has been clarified that various waves exist on Venus, but their spatial structures are not well understood. We focus on the periodical fluctuation of the cloud top temperature which has not been studied well.

We used images taken by the Long Infrared camera (LIR) onboard JAXA's Venus orbiter Akatsuki. LIR can capture the temperature of clouds around 65 km altitude. The image data taken by LIR has a systematic error of ˜3K and a relative error of ˜0.3K. Thanks to the small relative error of LIR, comparison of brightness temperatures in each image can be relatively accurate, and thus spatial inhomogeneities of the brightness temperature caused by waves are expected to be detectable. We focused on the longitudinal gradient of the brightness temperature. Considering the effect of limb-darkening, we focused on the same emission angles of the eastern and western side of the Venus disk in order to observe the brightness temperature coming from the same altitude. We calculated the averages of the brightness temperatures on the eastern and western side of the Venus disk (the range of the emission angle 40 degrees - 60 degrees) and the difference between the averages of the brightness temperatures. Longitudinal gradient of the brightness temperature is obtained by dividing the east-west temperature difference by the longitudinal distance between the two regions. The longitudinal gradient was arranged in time series and the periodicity was investigated by FFT analysis.

From FFT analysis, the brightness temperature fluctuation has several days periods. However, the influence of the change of the observed longitude due to spacecraft motion needs to be removed before exactly determining the wave periods. A preliminary result of this analysis will be presented.

Vertical propagation of the large stationary gravity waves in the Venus atmosphere

Takeru Yamada[1]; Takeshi Imamura[2]; Tetsuya Fukuhara[3]; Makoto Taguchi[1]
[1] Rikkyo Univ.; [2] The University of Tokyo; [3] Rikkyo Univ.

https://typememo.com/

The Longwave Infrared Camera (LIR) onboard Akatsuki detects thermal radiation from the cloud-top and derives a temperature distribution from an image obtained by LIR. A bow-shaped temperature structure with a meridional scale of about 10,000 km extending from Aphrodite Terra to the northern and southern polar regions was discovered by the observation by LIR just after the Venus orbit insertion. This temperature structure was located at the same position for four earth days at least, although the westward wind has a speed of 100 m/s. This temperature structure is interpreted as a stationary gravity wave excited by a flow over a mountain below the apex of the bow. In addition, it was found from the observation by LIR from December 7, 2015 to February 28, 2017 that similar temperature structures repeatedly appear above the mountains with a peak height of 5 km or higher and a width of 3 km or wider in the low latitude region when they are in the afternoon. Navarro et al. (2018) proposes an excitation mechanism of theses stationary gravity waves, which are generated by a diurnal cycle of static stability near the surface. The stationary gravity waves are reproduced by adapting the gravity wave stress to their general circulation model.

The finding of the stationary features at the cloud-tops means that the stationary gravity waves propagate vertically through the neutral layer existing at the altitudes of the cloud layer of the Venus atmosphere. Radio occultation measurements by Akatsuki showed that the thickness of the neutral layer is thicker in the morning (~10 km) than in the evening (~5 km) in the low latitude region. Bougher et al. (1997) mentioned the possibility of topographical gravity waves with horizontal wavelength longer than 100 km can propagate vertically through the neutral layer. However, detailed aspects have not yet been investigated.

We investigated how the gravity waves vertically propagate through the neutral layer by a numerical simulation using spherical sigma coordinate primitive equations developed by Imamura (2006) and Fukuhara et al. (2017). In the model the longitude and latitude are divided into 120 and 60 grids with an equal interval of 3 degree and the altitude range from 5 to 80 km is divided into 100 layers with a thickness of about 1 km. The basic wind field is longitudinally uniform. The zonal wind field is given to match the observation results. Furthermore, the meridional wind field is set to 0 to ignore the influence of meridional circulation. Assuming the cyclostrophic balance, the meridional temperature field is determined from the zonal wind field given as the basic field. To investigate the influence due to the difference in the thickness of the neutral layer in the local times, experiments were conducted by giving vertical profiles of the static stability with the different thicknesses of the neutral layer (0 km, 5 km, and 10 km) as initial states. To simulate terrain disturbance, we apply a two-dimensional Gaussian-function temperature forcing with an amplitude of 2 K and with a half-width of 6 degree at the altitude of 5 km centered at (180E, 0N) degree as the lower boundary condition. In our model, only the disturbance field evolves in time, and the basic field keeps its initial condition.

In order to compare the observation results of LIR and the simulation results under the same condition, the horizontal structure of the temperature disturbance obtained by the simulation is weighted by the weighting function of LIR and vertically integrated. As a result, the maximum temperature disturbance amplitude (MTDA) over the equator was 1.14 K for the cases of neutral layer thickness of 0 and 5 km. Even for the thickness of 10 km, MTDA is 0.85 K, which is sufficiently larger than the detection limit of LIR (= 0.3 K). This result shows that the stationary gravity waves can pass through the neutral layer, though the amplitude is damped more or less when passing through the neutral layer.

あかつき中間赤外画像の積算による金星雲頂の定在構造の抽出

福谷 貴一 [1]; 今村 剛 [2]; 田口 真 [3]; 福原 哲哉 [4]; 神山 徹 [5]
[1] 東大・理; [2] 東京大学; [3] 立教大・理・物理; [4] 立教大・理; [5] 産総研

Stationary features at Venusian cloud top extracted by averaging multiple mid-infrared images

Kiichi Fukuya[1]; Takeshi Imamura[2]; Makoto Taguchi[3]; Tetsuya Fukuhara[4]; Toru Kouyama[5]
[1] School of Science, Univ. of Tokyo; [2] The University of Tokyo; [3] Rikkyo Univ.; [4] Rikkyo Univ.; [5] AIST

The temperature distribution at the cloud top of Venus is observed by long-wave Infrared camera mounted in Venus orbiter "Akatsuki". Fukuhara et al. (2017) analyzed this observation data and reported the existence of arcuate features extending over 10,000 km in the north-south direction. The features are fixed in position without flowing with the superrotation and appear above highlands. It was suggested based on a comparison with numerical simulations that the features are stationary gravity waves. Kouyama et al. (2017) observed stationary features over 4 Venus days and revealed that the features tend to occur in the local afternoon.

Gravity waves, whose restoring force is buoyancy, transport momentum in the vertical direction and accelerate or decelerate the background wind when they dissipate. Therefore, stationary gravity waves influence the general circulation of the atmosphere. In order to estimate the influence, it is essential to reveal the spatial and temporal distributions of gravity waves.

In the previous studies using Akatsuki observations, only planetary-scale stationary features have been discussed. On the other hand, Peralta et al. (2017) analyzed the observation data of VIRTIS onboard Venus Express, and reported the existence of many small-scale stationary features. VIRTIS can observe the night side only, and the observations were confined to the southern hemisphere because of the geometry of the orbit. Therefore, we intend to investigate the topographical and local time dependency of small-scale stationary features by using Akatsuki LIR data, which can observe all the local time and both the northern and southern hemispheres. The S/N ratio of Akatsuki LIR is lower than VIRTIS, and thus it is difficult to capture small stationary features in each single image. Therefore, we analyzed LIR data by averaging multiple images to emphasize stationary patterns. By using this method, small stationary features could be visualized. In this presentation, we will report on this analysis result.

金星探査機「あかつき」のに搭載された中間赤外カメラにより雲頂高度における温度分布のデータが得られている。この観測データを解析した Fukuhara et al. (2017) では南北方向 1 万 km に渡る弓状の模様の存在が報告された。この模様は高地に現れ、スーパーローテーションの影響を受けずにほぼ同じ場所に留まることが明らかになった。また数値シミュレーションとの比較により地形性の重力波であることが示唆された。Kouyama et al. (2017) では 4 金星日に渡って弓状の模様を観測した結果、これらは毎金星日の特定の地方時によく発生する傾向があることが明らかになった。

重力波は浮力を復元力とする大気波動であり、運動量を鉛直方向に輸送するはたらきがあり、散逸することで平均風を加減速させる。ゆえに地形に固定された重力波は大気大循環に影響を及ぼす。その大きさを見積もるためには地形に固定された重力波の存在量の見積もりが必要不可欠である。

あかつきの観測を用いた先行研究では惑星規模の地形性重力波のみが議論されてきた。一方で Peralta et al. (2017) では VIRTIS（Venus Express）の観測データを解析することで、より小規模な地形に固定された構造が多く存在することが報告された。VIRTIS（Venus Express）はその特性から夜側、南半球しか観測ができない。そこで私たちは南北両半球の全てのローカルタイムを観測可能なあかつき LIR の観測データを用いることで、小規模な地形に固定された構造を調査しそれらの地形、地方時依存性を調べることを試みた。あかつきの中間赤外線カメラは VIRTIS（Venus Express）と比べ S/N 比が低いため、1 枚の画像データを解析して小規模な構造を捉えることが困難である。そこでハイパス処理を施した画像を複数枚平均することで地形に固定された構造を強調させる方法を用いて画像を解析した。この手法により、個別の画像では判別できない小振幅の地形固定構造を可視化することができた。本発表ではこの解析結果について報告する。

Comparison of horizontal distributions of temperature and UV absorbers at the Venus cloud-tops

Shinichiro Kawase[1]; Makoto Taguchi[2]; Tetsuya Fukuhara[3]
[1] Physics, Rikkyo Univ.; [2] Rikkyo Univ.; [3] Rikkyo Univ.

Venus is the nearest neighbor planet, which has a size similar to that of the earth. However, unlike the earth, Venus is covered with thick H_2SO_4-H_2O clouds floating at 45-70 km altitudes [Nakamura et al., 2011]. It is considered that the clouds are photochemically generated by oxidation of SO_2 and H_2O. In the visible region, light reflected by the clouds are poorly absorbed and few structures are noticeable. On the other hand, in the ultraviolet (UV) region, inhomogeneity of albedo has been identified to be inhomogeneous distribution of UV absorbers above the layer of UV scattering. It has been identified that SO_2 in the Venusian atmosphere absorbs light in the wavelength region between 200 nm and 320 nm, but chemical species responsible for the absorption in the wavelength region longer than 320 nm is still unidentified. S_2O and OSSO are candidates. The UV absorbers play an important role in the atmospheric dynamics, controlling vertical thermal stability by heating at the top of convection layer. The dynamics may feedback the distribution of the UV absorbers by transport of them from the lower atmosphere. Details of the chemical and dynamical coupling are still unknown.

Images obtained by the Longwave Infrared Camera (LIR) and Ultraviolet Imager (UVI) onboard the Venus orbiter Akatsuki were analyzed. LIR takes images of thermal radiation in the wavelength range of 8-12 um emitted from the cloud-tops [Fukuhara et al., 2011]. Temperature distributions are derived from the images. Disturbances seen in the temperature distributions are thought to be caused by atmospheric waves and tides, changes in the cloud-top altitude and adiabatic heating and cooling due to convection, direct heating by the UV absorbers, and so on.

UVI takes images of the solar radiation reflected by the clouds with narrow bandpass filters centered at the 283 and 365 nm wavelengths, which correspond to the absorption bands of SO_2 and unknown absorbers [Yamazaki et al., 2018].

We compared horizontal distributions of the temperature and UV absorbers, and examine correlation between them. Examples are shown in Figure. Correlation coefficients were calculated for square regions of 1.2 degree by 1.2 degree. In the temperature distribution, a bright (high temperature) pattern is seen around 50 degree south. It is found that there are strong positive correlations in this region. However, there are positive correlations up to around 60 degree south. It is considered that the UV absorbers do not change in concentration and are along the cloud tops despite the fact that the temperature (altitude) of the cloud tops change in this region.

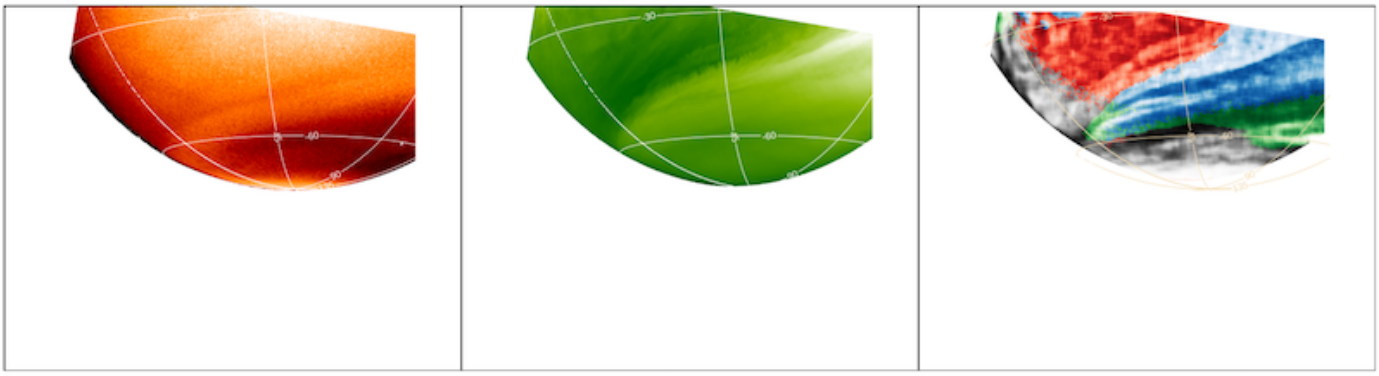

Cloud top altimetry of Venus with Akatsuki/IR2 dayside images

Takao M. Sato[1]; Takehiko Satoh[2]; Hideo Sagawa[3]; Naohiro Manago[4]; Yeon Joo Lee[5]; Shin-ya Murakami[1]; Kazunori Ogohara[6]; Yasumasa Kasaba[7]; Masato Nakamura[8]
[1] ISAS/JAXA; [2] ISAS, JAXA; [3] Kyoto Sangyo University; [4] CEReS/Chiba Univ.; [5] JAXA/ISAS; [6] JAXA/ISAS; [7] Tohoku Univ.; [8] ISAS

We have analyzed a total of 93 Venus' dayside images taken by the 2.02-micron channel of 2-micron Camera (IR2) onboard Japanese Venus orbiter, Akatsuki, during the period from April 4 to May 25, 2016 (Orbits 12-16), for the purpose of mapping cloud top altitude. Since the 2.02-micron channel locates in a CO_2 absorption band, the observed brightness contrast is interpreted as resulting from the difference of the optical path length to the cloud top: the cloud top altitude can be retrieved by reproducing the observed radiance with radiative transfer calculation. We first investigated the observed phase curve (solar phase angle dependence of the radiance) for the equatorial region to constrain the averaged cloud top structure characterized by cloud top altitude (z_c), cloud modal radius (Mode 2, $r_{g,2}$), and cloud scale height (H). The best-fit model was obtained at the combination of z_c=70.3 km, $r_{g,2}$=1.07 micron, and H=5.1 km. Once the best-fit combination of $r_{g,2}$ and H was determined, as the second step, we retrieved cloud top altitude maps under the assumptions that the pixel-to-pixel radiance variation arises as the deviation from the averaged cloud top structure and can be explained by the change of the cloud top altitude while keeping the other parameters ($r_{g,2}$ and H) unchanged. The average of zonally-averaged cloud top profiles was found to be symmetrical with respect to the equator. The averaged cloud top in the low and middle latitudes ($<$45 deg) exists in altitude of 68-70 km. It rapidly decreases in latitudes of 50-60 deg and reaches 61 km poleward of 70 deg. This global pattern is consistent with the previous studies with Venus Express data.

主成分分析を用いた金星の雲形態からの特徴抽出

成田 穂 [1]; 今村 剛 [2]; 奈良 佑亮 [3]; Lee Yeon Joo[4]; 渡部 重十 [5]; 山崎 敦 [6]; 佐藤 毅彦 [7]; 田口 真 [8]; 福原 哲哉 [9]; 山田 学 [10]
[1] 東大・新領域・複雑理工; [2] 東京大学; [3] 東大・新領域; [4] JAXA/ISAS; [5] 北大・理・宇宙; [6] JAXA・宇宙研; [7] 宇宙研; [8] 立教大・理・物理; [9] 立教大・理; [10] 千葉工大・惑星探査研究センター

Feature extraction from Venusian cloud morphology using principal component analysis

Minori Narita[1]; Takeshi Imamura[2]; Yusuke Nara[3]; Yeon Joo Lee[4]; Shigeto Watanabe[5]; Atsushi Yamazaki[6]; Takehiko Satoh[7]; Makoto Taguchi[8]; Tetsuya Fukuhara[9]; Manabu Yamada[10]
[1] none; [2] The University of Tokyo; [3] GSFS, Univ. Tokyo; [4] JAXA/ISAS; [5] Cosmosciences, Hokkaido Univ.; [6] ISAS/JAXA; [7] ISAS, JAXA; [8] Rikkyo Univ.; [9] Rikkyo Univ.; [10] PERC/Chitech

We analyzed Venusian images taken from Venus orbiter Akatsuki using principal component analysis for each wavelength, and successfully extracted spatial patterns characteristic to each wavelength. We also statistically compared the similarity and the dissimilarity between wavelengths. It turned out that lateral (zonally-aligned) streaky features were dominant in every wavelength analyzed and that patchy fine features had smaller contribution ratios than streaky features. Differences were seen between wavelengths as described below.

We preprocessed images as follows. We used data in which images have been projected onto the latitude-longitude coordinate (Level-3 data), and as for the wavelengths, near-infrared 2 um, thermal infrared 10 um, ultraviolet 283 nm, and ultraviolet 365 nm were chosen. Near-infrared 2 um reflects the cloud height, thermal infrared 10 um corresponds to the cloud top temperature, ultraviolet 283 nm shows the distribution of SO_2 at cloud top, and ultraviolet 365 nm shows the distribution of unknown UV absorbers. First, the large-scale brightness variation due to the change of the incidence and emission angles over the Venus disk was removed by using Minnaert law (except for thermal infrared 10 um images). Then these images are processed by high-pass filtering by subtracting a Gaussian-smoothed image from each original image, and features which have scales smaller than 6 degrees in latitude/longitude are extracted. Lastly, we divided images into patch images to increase the number of samples and extract specific spatial scale. The size of a patch image has 12 degrees in latitude/longitude, and the patch images were taken from the valid region in each high-pass filtered image. The total number of patch images was around 70,000 for each wavelength.

We executed principal component analysis for patch images described above. Principal component analysis converts a set of observational data into a set of values of linearly uncorrelated variables called principal component and enables to reduce the dimensionality of the data and extract spatial features that appear in data frequently. We computed up to the twentieth principal component for each wavelength, and we also calculated the contribution ratios. As a result, lateral streaky features are found to be dominant in all wavelengths analyzed, and the contribution ratio of vertical streaky features and patchy structures were relatively small. It was also found that lateral streaky features prevail more in middle latitudes than in low latitudes. Moreover, it turned out that there is a strong similarity between the principal components in ultraviolet 283 nm and 365 nm, and that the first principal component in thermal infrared 10 um has smaller contribution ratio than the other wavelengths.

Next, we applied principal component analysis to a combined data set of ultraviolet 283 nm and 365 nm and studied the difference of the variance of principal component coefficients between the wavelengths. It was shown that the data of ultraviolet 365 nm show larger variances than the data of 283 nm for components with small contribution ratios. This suggests that 365 nm has more complicated spatial structures than 283 nm. Lastly, we compared principal components between the morning side and the afternoon side in thermal infrared 10 um. From the result, it turns out that vertical stripe-like features are predominant in part of the images in the afternoon region, and that those images correspond to the area in which stationary features appear. The result supports the previous analysis that stationary features tend to appear on the afternoon side. Similar analyses are ongoing for the other wavelengths such as 2 um, 283nm, and 365 nm.

金星探査機あかつきにより得られた金星画像を用いて波長ごとに主成分分析を行うことで、それぞれの波長に特有の空間パターンを抽出し、また波長間の類似性や相違性について統計的に比較した。その結果、いずれの波長においても横縞が卓越することや、粒状の細かい構造の寄与率は筋状の構造に比べ小さいことが分かった。また、波長ごとの特性についても、後述するように違いが見られた。

主成分分析を行う前に、各画像について以下のように前処理を行った。解析には金星画像を緯度経度に展開したマップ（Level-3 データ）を使用し、近赤外 2 μ m、中間赤外 10 μ m、紫外線 283 nm、紫外線 365 nm の 4 波長について解析を行った。近赤外 2 μ m は雲頂高度、中間赤外 10 μ m は雲頂温度、紫外線 283 nm は雲頂の SO_2 分布、紫外線 365 nm は雲頂の未知の紫外線吸収物質の分布をそれぞれ反映している。まず、太陽の入射角および出射角依存性を取り除くため、中間赤外 10 μ m を除く 3 波長について Minneart Law を用いて輝度値の補正を行った。次に画像に対してガウシ

アンフィルタを用いてぼかした画像と元画像との差分を取ることでハイパスフィルタリングを行い、緯度経度 6 度分以下の小さな構造のみを抽出した。最後に、サンプル数の増加および特定の空間スケール抽出のために、各画像を細かなパッチ画像に分割した。一枚のパッチ画像の大きさは緯度経度 12 度分とし、各ハイパス画像の全有効値領域に対して切り出しを行った。パッチ画像の総数は波長ごとにそれぞれ 70,000 枚前後となった。

上で説明したパッチ画像群に対して主成分分析を行った。主成分分析は観測データを線形的に無相関な主成分に変換し、これによりデータの次元を削減してデータによく現れる空間的特徴を抽出することが可能になる。画像群により強く表れる特徴的パターンほど寄与率の高い成分として先に現れる。上で述べた 4 波長について第 20 主成分まで算出し、それぞれの寄与率も計算した。その結果、全ての波長において横方向 (東西方向) の縞模様が支配的になり、縦縞あるいは粒状の構造の寄与率は比較的低くなることが分かった。また、中緯度の方が低緯度よりも横縞 (東西方向の縞) が卓越することが分かった。さらに、紫外線 283 nm、紫外線 365 nm の主成分の間に強い類似性があること、中間赤外 10 μ m の第一主成分の寄与率が他の波長に比べ小さいことが分かった。

次に、紫外線 283 nm、紫外線 365 nm のパッチ画像をまとめて主成分分析し、その後波長ごとの主成分の係数の分散の違いを調べた。その結果、紫外線 365 nm の方が紫外線 283 nm に比べて寄与率の小さな成分まで分散が大きいことが分かった。これは 365 nm の方が 283 nm に比べて複雑な空間的構造を持つことを示している。最後に、中間赤外 10 μ m について午前側と午後側の主成分を比較した。結果を見ると、午後側の一部の画像で縦縞の成分が大きく卓越しており、これは地形固定構造の出現箇所に対応していることが分かった。これは午後側に地形固定構造が現れる傾向があるという従来の解析を裏付ける結果となった。他の波長でも同様の解析が進行中である。

あかつき電波掩蔽により見出された金星大気の地方時依存構造

今村 剛 [1]; 安藤 紘基 [2]; 野口 克行 [3]
[1] 東京大学; [2] 京産大; [3] 奈良女大・理・環境

Localtime-dependent structures in the Venusian atmosphere revealed by Akatsuki radio occultation measurements

Takeshi Imamura[1]; Hiroki Ando[2]; Katsuyuki Noguchi[3]
[1] The University of Tokyo; [2] Kyoto Sangyo University; [3] Nara Women's Univ.

As the localtime-dependent structure in the Venusian atmosphere, structures that seem to be thermal tides have been detected in the wind field at the cloud top and in the atmospheric temperature above the cloud layer; however, localtime-dependent structures below the cloud top are unknown. The cloud-level atmosphere undergoes a periodical change in solar heating with a period of about 4 days due to the super rotation. It is expected that this affects cloud physics through a periodic variation of convection in the cloud layer (Imamura et al. 2016), although it has not been observed. It is reported that disordered patterns are seen at the cloud top especially in the vicinity of the sub-solar point, but what kind of temperature fluctuation causes it is unclear. Thermal tides may contribute to the maintenance of the super rotation, and it is particularly important that thermal tides propagate downward below the cloud layer to carry momentum, but the structure of the waves below the clouds is not known.

Radio obscuration is a powerful technique to capture such atmospheric variations below the cloud top. We have conducted radio occultation measurements from 2016 using Venus orbiter Akatsuki, and have acquired temperature and pressure profile. Since the spacecraft is orbiting the equatorial region, data were obtained especially in the low latitude. According to the initial analysis, the thickness of the neutral layer in the cloud seems to be thicker and more variable on the nightside than on the dayside. This is considered to reflect the variation of the convection intensity. Structures depending on the localtime are seen also below the cloud layer; they might be related to thermal tides. Above the cloud layer, we observe structures finer than the wavenumber-1 and 2 components that were conventionally recognized as thermal tides. We discuss implications of those structures in this presentation.

金星では地方時に依存する大気構造として、雲頂の風速分布や雲層より上の大気温度に熱潮汐波と思われる構造が検出されているが、それより低高度にどのような地方時依存構造があるのかはわかっていない。雲層高度の大気はスーパーローテーションによって約4日の周期で太陽光加熱の変化を受ける。そのことが雲層内の対流の周期変動を通じて雲物理に影響を与えることが予想されているが (Imamura et al. 2016)、観測では捉えられていない。雲を紫外線で撮像すると太陽直下点付近でとくに乱れた模様が見られることが報告されているが、これが大気温度のどのような変動によって引き起こされるのかもわかっていない。熱潮汐波はスーパーローテーションの駆動に関わる可能性があり、とくに雲層以下に伝播する熱潮汐波が下層大気との間で運動量を運ぶことが重要であるが、雲より下での伝播の様子はわかっていない。

このような雲頂以下の大気変動をとらえる有力な手法として電波掩蔽がある。我々は金星探査機「あかつき」を用いて2016年から電波掩蔽観測を行い、気温・気圧プロファイルを取得してきた。探査機が赤道周回しているため、とくに低緯度で多くの観測データが得られており、この領域で地方時依存性を調べることが可能になりつつある。初期的な解析によれば、雲層内にある中立層の厚みが昼側より夜側で厚く、変動が大きいように見える。これは対流強度の変動を反映するものと考えられる。雲層以下でも地方時に依存する構造が見られており、熱潮汐波を検出した可能性がある。雲層より上においては、従来熱潮汐波として認識されていた東西波数1、2の成分よりも細かい構造が見られるようである。本発表ではこれらの構造について議論する。

惑星大気観測ビッグデータ解析に向けた放射伝達計算コードARTSの拡張

菅原 徹也 [1]; 平原 靖大 [2]
[1] 名大・環; [2] 名大・院・環境・地球惑星

Extension of the radiative transfer code ARTS for big data analyses of planetary atmosphere

Tetsuya Sugawara[1]; Yasuhiro Hirahara[2]
[1] Environmental studies, Nagoya Univ.; [2] Earth&Planetary Sciences, Nagoya Univ.

Radiative transfer is the most important factor in interstellar and atmospheric sciences. The forward model which deduces the intensity of radiation based on the various information such as the pressure, temperature and molecular abundance in the atmosphere enables us to develop and design a new instrument and to add the constraint to the observed results by comparing with the simulated results. Along with the improvement of remote sensing and ground observation technology, the accuracy and calculation speed required for the radiative transfer code are also increasing. In particular, planetary science has entered a new generation since the beginning of the operation of ALMA telescope. However, there is a problem that large amounts of observed data are currently being buried as the archive data. So it is needed to develop a new, high resolution and convenient code to resolve and identify the detailed 3D structure of the atmosphere.

In this study we improved the radiative transfer code for general planetary atmosphere based on ARTS (the atmospheric radiative transfer simulator; Buehler et al. 2018). ARTS is a radiative transfer package which is suitable for a wide wavelength region, mainly for the millimeter and sub-millimeter region. According to the recent study of the intercomparison of some latest radiative transfer codes (Schreier et al. 2018), ARTS showed sufficient results in the brightness temperature region as the Earth (215<=T_B<=300 K). We performed a simulation of HC_3N in the Titan, the well-known moon of Saturn based on ALMA archive data from our interest. It is found that ARTS had some problems with simulation in the case of low-temperature atmosphere (T_B~100 K). Besides that, to our knowledge, study reports with ARTS applied to general objects other than the Earth have not been done yet. Then we will present the implementation of ARTS which enables to apply the radiative transfer analysis to the Titan atmosphere as an example.

放射伝達計算は宇宙科学や大気科学において最も重要な要素である。その中で大気の圧力、温度、構成元素の存在度など各種情報に基づいて実際に測定されうる放射強度を計算するフォワードモデルは、次代の観測機器の開発と設計に新たな知見をもたらすほか、実際の観測データとシミュレーション結果を照らし合わせることでこれまでの観測結果に制約を加えることができる。しかし、リモートセンシングと地上観測両技術の向上に伴い、放射伝達計算を行うコンピューターコードに要求される精度や計算速度も比例して大きくなってきている。特に、最近はアルマ望遠鏡の登場により惑星科学は新しい時代へ突入したものの、解析速度が観測に追いついておらず、観測データが大量のアーカイブデータとしてうずもれてしまっていることは大きな問題である。そこでアルマ望遠鏡以上に大気の3次元構造を詳細に分離・検知できるような、高分解能で高速処理が可能な便利で新しいコードの開発が急務になっている。

本研究は大気放射伝達シミュレーター ARTS (Buehler et al. 2018) をベースに、一般的な惑星大気で放射伝達計算が可能なコードへの拡張・開発を行う。ARTS はミリ波・サブミリ波領域を中心に、広範な波長領域に対応した放射伝達コードである。最新の放射伝達コードを相互比較した研究では、ARTS は地球ほどの輝度温度 (215 $\leqq$ T_B $\leqq$ 300 K) の場合十分に精緻な結果が得られた (Schreier et al. 2018)。しかし我々の研究室の興味によりアルマアーカイブデータを解析して得た土星の衛星タイタンの大気中に微量に存在する HC_3N に関してシミュレーションを行ったところ、ARTS は低温大気 (T_B~100 K) での計算に問題があることが分かった。さらに、現時点で ARTS を用いて地球以外の天体についてシミュレーションした研究報告はいまだ為されていない。そこで本発表ではタイタン大気を例にとり、改良・拡張開発したコードと ARTS の比較を行い、シミュレーションした結果について議論する。

中間赤外線観測装置のための冷却中空ファイバーガイドの開発

伊藤 良太 [1]; 平原 靖大 [2]; 青木 翔平 [3]; 中川 広務 [4]; 笠羽 康正 [5]
[1] 名大・環; [2] 名大・院・環境・地球惑星; [3] BIRA-IASB; [4] 東北大・理・地球物理; [5] 東北大・理

Development of cooled hollow core waveguide for mid infrared observing instruments

Ryota Ito[1]; Yasuhiro Hirahara[2]; Shohei Aoki[3]; Hiromu Nakagawa[4]; Yasumasa Kasaba[5]
[1] Environmental Studies, Nagoya Univ.; [2] Earth&Planetary Sciences, Nagoya Univ.; [3] BIRA-IASB; [4] Geophysics, Tohoku Univ.; [5] Tohoku Univ.

We aim at the long-term observation of the planetary atmosphere in the mid-infrared wavelength region for the purpose of clarifying various phenomena of atmosphere physics and atmospheric chemistry of solar system planets and satellites for by 1.8m off-axis telescope PLANETS(Polarized Light from Atmospheres of Nearby Extra-Terrestrial Systems), which is planned to be constructed at Mt. Haleakala of Maui, equipped with high dispersion cooled echelle spectrograph GIGMICS(Germanium Immersion Grating Mid-Infrared Cryogenic Spectrograph), which can observe N-band(wavelength 8~13 micro-meter) with R~40,000. In this research we report the development of the new cooled fiber system for optical guiding to GIGMICS from PLANETS. By using the mid infrared HCW(hollow core waveguide) developed in recent years, we can realize simultaneous observation with other observing instruments such as MILAHI, and improvement of optical throughput by abbreviation of a large number of guide mirrors.

It is needed for operation to cool the HCW for suppression of thermal radiation from HCW itself, and to sealing for vacuum. Accordingly, we designed fabricated, and examined the sealing and coupling mechanism for both end face of fiber (~1mm diameter) by germanium micro lenses. We also designed the double insulation Wilson seal for connection of end face of fiber and entrance window of GIGMICS. The new Wilson seal can cool HCW inserted in the OFHC (Oxygen-Free High-Conductivity) Copper sleeve by the internal cooling system of GIGMICS, and vacuum sealed by using o-ring or metal gasket. We are now verifying the performance.

多様な太陽系惑星・衛星の大気物理・大気化学の諸現象を観測的に明らかにする目的で、我々は、マウイ島ハレアカラ山頂に建設予定の 1.8m 軸外し型グレゴリアン式望遠鏡 PLANETS(Polarized Light from Atmospheres of Nearby Extra-Terrestrial Systems) に、赤外線領域の「大気の窓」である N-band(波長 8~13 micro-meter) 全域を観測域とする高分散 (R~40,000) 冷却エシェル分光器 GIGMICS(Germanium Immersion Grating Mid-Infrared Cryogenic Spectrograph) を搭載することで、中間赤外域での惑星大気の連続的な観測を目指している。本研究では、GIGMICS を PLANETS に搭載・運用するための新型のファイバーの開発について報告する。近年において開発された中間赤外線中空ファイバーを用いて光学的に接続することで、MILAHI など、他の観測装置との併用が可能になるとともに、多数のガイドミラーの省略により、光学的なスループットの向上が達成でき、その結果として、分子スペクトルの検出感度を大幅に向上できる。

中間赤外ファイバーによる望遠鏡との接続を実用化するためには、ファイバー自身からの熱放射を抑えるための冷却と、空気の流入を防ぐための真空シーリングが必要となる。そこで我々は、(1) ファイバー端面 (~1mm ϕ) のゲルマニウムマイクロレンズによるカップリングとシーリング機構。(2) ファイバー端面と GIGMICS 入射窓との接続のための二重断熱ウィルソンシールの仕様検討・機械設計と製作を行った。(1) については、真空冷却試験の結果、良好な性能を確認できた。(2) の新型ウィルソンシールでは、ファイバーを薄い無酸素銅スリーブを介して o-ring もしくはガスケットで真空保持しつつ、GIGMICS の冷却系により直接冷却可能な新機構とした。今後の動作試験により、その性能を検証する。

あかつきで観測された電波シンチレーションと気温擾乱の関係

出原 千裕 [1]; 野口 克行 [1]; 安藤 紘基 [2]; 今村 剛 [3]; Tellmann Silvia[4]; Paetzold Martin[4]; Haeusler Bernd[5]
[1] 奈良女大・理・環境; [2] 京産大; [3] 東京大学; [4] ケルン大; [5] ドイツ・ミュンヘン連邦軍大

Relationship between radio scintillation and temperature perturbation in the Venusian atmosphere observed by Akatsuki

Chihiro Idehara[1]; Katsuyuki Noguchi[1]; Hiroki Ando[2]; Takeshi Imamura[3]; Silvia Tellmann[4]; Martin Paetzold[4]; Bernd Haeusler[5]
[1] Nara Women's Univ.; [2] Kyoto Sangyo University; [3] The University of Tokyo; [4] Univ. Cologne; [5] UniBwM

Radio scintillation is caused by atmospheric refractivity irregularities, which are related to atmospheric number density perturbations. We analyzed 18 profiles obtained by Akatsuki radio occultation measurements since March 2016. We found that Low stability regions (in clouds) had small temperature perturbation (T') and scintillation (I') while high stability regions (above/below clouds) had larger T' and I'. Those results were consistent with previous Magellan observations [Hinson and Jenkins 1995, Icarus]. However, a large T' appeared around the altitudes of 80-90km, which was not found in the Magellan measurements.

電波シンチレーションは、電波が大気を通過する際に、大気数密度擾乱に伴う屈折率の不規則構造によって電波強度が短い時間スケールで変動する現象である。金星探査機あかつきによる電波掩蔽観測では、雲層の上下の高度領域において、電波シンチレーションと共に鉛直波長が数 km 程度の気温擾乱も多く観測された。一方で、雲層のある高度域では大きな気温擾乱は見られず、電波シンチレーションの強度も小さくなっていた。このような関係は、Hinson and Jenkins [1995, Icarus] でも述べられており、金星探査機マゼランによる観測結果と整合的である。ただし、高度約 80〜90km では、振幅の大きい気温擾乱が観測されているにも拘らず、電波シンチレーションはほとんど発生していなかった。マゼランによる観測では、高高度においてこのように大きな気温擾乱自体が報告されていないため、今後さらに詳細な解析を行う予定である。

金星大気の鉛直温度分布のウェーブレット解析

森 亮太 [1]; 今村 剛 [2]
[1] 東大・新領域・複雑理工・アストロバイオ; [2] 東京大学

Wavelet analysis of temperature profiles of the Venus atmosphere

Ryota Mori[1]; Takeshi Imamura[2]
[1] Astrobio,Complexity Science and Engineering,Frontier Sciences, Tokyo Univ; [2] The University of Tokyo

Temperature profiles has been obtained from 2016 by the radio occultation experiment in the Venus orbiter mission Akatsuki. The radio occultation experiment is a method that measures the change of the atmospheric refractive index as a change of the frequency of the signal received on the ground. At the opportunity when the radio wave transmitted from Akatsuki toward the Earth pass through the planetary atmosphere, the wave is refracted and then reaches the receiving station. We can retrieve the vertical profiles of the pressure and the temperature from each refractive index profiles. In the temperature profile obtained in this way, variations due to various atmospheric disturbances are observed. We focus on gravity waves which are thought to play an import role in driving the general atmosphere circulation.

Gravity waves are small-scale waves with the restoring force being the buoyancy in the atmosphere. Gravity waves play a role in carrying the momentum in the vertical direction. So, it results in acceleration or deceleration of the mean wind by passing momentum on the background atmosphere while dissipating. This process should affect the global structure of the high-speed zonal wind. However, since gravity waves have properties that the spatial scale is small and the wave period is relatively short, it is difficult to capture the spatial structure by observation. The latitudinal profile of the amplitude of short vertical-scale temperature disturbances, which are thought to be associated with gravity waves, has been investigated; however, the dominant wavelength and the typical vertical extent have not been studied.

In this study, we applied wavelet analysis to the temperature profiles and extracted spatially localized temperature disturbances. Though there have been studies that apply Fourier transform to the temperature data, Fourier transform assumes infinitely lasting waves and it is not suitable for extracting spatially localized wave packets. Wavelet analysis is an effective way of obtaining the periods and the amplitudes of waves in such finite intervals. In this presentation, we report the result of wavelet analysis applied to the temperature data obtained with high vertical resolution by radio holographic method.

金星探査機「あかつき」の電波掩蔽観測により 2016 年から現在に至るまで大気温度の高度分布が得られている。電波掩蔽観測は、探査機から送信される電波が惑星大気を通過して屈折したのち地球の受信局に届く機会を利用して、大気の屈折率の変化を地上での受信周波数の変化として捉える手法であり、屈折率の高度分布から気圧や気温を導出することが出来る。こうして得られる気温分布には様々な大気擾乱に起因する変動が観測される。ここでは、大気大循環の駆動において重要な役割を持つと考えられる大気重力波に注目する。

重力波は大気中の浮力を復元力とする小規模な波動である。重力波は運動量を鉛直方向に運ぶ働きがあり、散逸に際して背景大気に運動量を受け渡すことにより、平均風の加減速をもたらす。金星においては高速帯状風の全球的な構造に影響を与えていることが予想されている。しかし、重力波は空間スケールが小さく、周期が比較的短いという性質があるために、その空間構造を観測で捉えることが難しい。これまでに、重力波に伴うと考えられる短鉛直波長の温度擾乱の振幅の緯度-高度分布などが調べられてきたが、卓越する波長や高度方向の拡がりについては分かっていなかった。

そこで、本研究では、ウェーブレット解析を鉛直温度分布に適用し、空間的に局在した温度擾乱を抽出する。今までは、温度データにフーリエ変換を適用した研究はあるが、フーリエ変換は無限に続く波を仮定としており、空間的に局在した波束の特徴を取り出すのには適切ではない。ウェーブレット解析はそのような有限区間の波に関して周期や振幅を得たい時に有効である。本発表では電波ホログラフィという方法で従来より高い高度分解能で得られた温度データに対してウェーブレット解析を適用した結果を報告する。

あかつき搭載IR1から明らかにする金星下層雲全球変動

高木 聖子 [1]; あかつき IR1 チーム 岩上　直幹 [2]
[1] なし; [2] -

The global variation of Venus' lower clouds obtained from IR1 camera onboard AKATSUKI

Seiko Takagi[1]; Iwagami Naomoto AKATSUKI IR1 team[2]
[1] Hokkaido Univ.; [2] -

Venus is our nearest neighbor, and has a size very similar to the Earth's. However, previous observations discovered an extremely dense (92 bar at the surface) and CO_2-rich atmosphere, with H_2SO_4 thick clouds. The Venus cloud consists of H_2SO_4 main cloud deck at 47 - 70 km, with thinner hazes above and below. The upper haze on Venus lies above the main cloud surrounding the planet, ranging from the top of the cloud (70 km) up to as high as 90 km.

Near infrared (0.986 um) dayside image of Venus has taken by solid state imaging (SSI) of the Galileo spacecraft (NASA). It appears almost flat, there are some small scale features with a contrast of 3 % [Belton et al., 1991]. In Takagi and Iwagami. (2011), it may be calculated that the source of the contrast of the order of 3 % in near infrared Venus dayside image is due to variation in the cloud optical thickness.

On December 7, 2015, AKATSUKI (JAXA) approached Venus and the Venus orbit insertion was successful. After the Venus orbit insertion, many 0.90 um Venus dayside images were taken by the 1 um near infrared camera (IR1) onboard AKATSUKI.

In this study, lower cloud variations are investigated from 0.90 um Venus dayside images taken by IR1 camera globally. Further, meteorological some changes that contribute to cloud variation are examined.

金星は地球とほぼ同じ大きさ・密度を持ち、太陽系形成時には互いに似た惑星として誕生したと考えられているが、90気圧もの二酸化炭素大気や全球を一様に覆う硫酸雲の存在など地球とは全く異なる様相を見せる。

金星探査機あかつき (JAXA) は、2015年12月に金星周回軌道投入に成功した。あかつきは複数波長による撮像観測を行い、金星気象の3次元的理解を目指す。搭載された近赤外カメラIR1は、軌道投入後約1年間、近赤外波長0.90 umにおける金星昼面撮像を行った。大気の窓領域である近赤外波長を用いた金星昼面撮像観測では、雲の光学的厚さの増減を金星表面のコントラストとしてとらえることができる [Takagi and Iwagami. 2011]。木星探査機 Galileo/SSI (NASA) により得られた金星昼面近赤外画像 (0.986 um) では、金星表面のコントラストはわずか3 %と示されている [Belton et al., 1991] が、IR1はかつて木星探査機 Galileo/SSI が得たものと整合的な昼面画像を多数取得している。

本研究では、IR1が取得した0.90 um昼面画像から下層雲の変動傾向を全球的に知る。また、雲変動に寄与する金星の気象変化について考察する。

Temperature and Wind variations in Venusian mesosphere and lower thermosphere by mid-infrared heterodyne spectrometer in 2018

Kosuke Takami[1]; Hiromu Nakagawa[1]; Hideo Sagawa[2]; Isao Murata[3]; Yasumasa Kasaba[4]
[1] Geophysics, Tohoku Univ.; [2] Kyoto Sangyo University; [3] Environmental Studies, Tohoku Univ.; [4] Tohoku Univ.

Venusian upper atmosphere is mainly classified into the mesosphere (70 - 100 km) and the thermosphere (100 km -). Large spatial and temporal variation of temperature profile in this region which had been believed stable was found by Venus Express (Tellmann et al., 2009). On the other hand, Venus has global circulations over 100 m/s which are a retrograde superrotaional zonal wind at the cloud top and a subsolar-to-antisolar circulation in the lower thermosphere. General Circulation Model (GCM) expected a wind shear by global circulations to complicate atmospheric profile in this region by generating the gravity waves (Rodin et al., 2013). The previous studies by mid-infrared (MIR) heterodyne spectrometer showed discrepancies with GCM and intense temporal variations of temperature (40 K) and wind velocity (30 m/s) (Sornig et al., 2013; Krause et al., 2018). These nature in the Venusian upper atmosphere are not understand comprehensively due to lack of continuous monitoring because the previous observations were conducted by competitive large telescopes.

Mid-Infrared Laser Heterodyne Instrument (MILAHI) is MIR heterodyne spectrometer developed by Tohoku University (Nakagawa et al., 2016). This instrument is attached to Tohoku University 60 cm telescope located at the summit of Mt. Haleakala. The advantage of this instrument is to conduct continuous observation by using the dedicated telescope. Sensitive altitude ranges of MIR heterodyne observation are different between a dayside observation and a nightside observation. A dayside observation is to obtain CO_2 10 um non-local thermodynamic equilibrium (non-LTE) emission generated from 100 - 120 km altitude in the lower thermosphere (Lopez et al., 2011). Kinetic temperature and wind velocity along line of sight are derived from line width and doppler shift, respectively (Sonnabend et al., 2008; Sornig et al., 2008). The CO_2 10 um absorption of the atmosphere upon the cloud top is observed in the nightside. We can retrieve temperature profile and wind velocity along line of sight between 70 km and 100 km in the nightside mesosphere by AMATERASU include a clear sky radiative transfer model, a receiver simulator and an inversion code (Takami et al., in preparation).

We conducted continuous observation of 8 days in June 2018. This observation campaign was dayside observation, so observed altitude was 100 - 120 km. Venusian evening terminator was coming to disk center in June 2018. We could divide Venusian dayside into 4 regions: disk center, equator limb, north high latitude and south high latitude due to field of view of 4 arcsec (MILAHI) and the apparent diameter of 13 arcsec (Venus). A latitude dependence was not found in this observation campaign and the results of temperature showed different variation features among observed regions. The average temperature decreased by 30 K from June 20th and increased by 40 K up to 220 K from 23th. The retrieval of wind velocity is under evaluation process.

We plan observation for nightside in October 2018 at just before inferior conjunction. This observation results will be shown. This study is the first time for derivation of wind velocity in Venusian mesosphere by remote sensing from ground-based observation.

金星大気大循環モデルを用いた金星雲物理に関する理論的研究

安藤 紘基 [1]; 高木 征弘 [2]; 杉本 憲彦 [3]; 佐川 英夫 [4]; 松田 佳久 [5]
[1] 京産大; [2] 京産大・理; [3] 慶大・日吉物理; [4] 京都産業大学; [5] 東京学芸大

Theoretical study of the Venusian cloud physics by a general circulation model

Hiroki Ando[1]; Masahiro Takagi[2]; Norihiko Sugimoto[3]; Hideo Sagawa[4]; Yoshihisa Matsuda[5]
[1] Kyoto Sangyo University; [2] Faculty of Science, Kyoto Sangyo University
; [3] Physics, Keio Univ.; [4] Kyoto Sangyo University; [5] Tokyo Gakugei Univ.

By using the Venusian general circulation model, the distributions of the cloud and condensable gases (H_2O and H_2SO_4 vapors) were reproduced. The numerical calculation is conducted on the following assumptions; the cloud is composed of Mode 1 with the radius of 0.5um and Mode 2 with that of 1.0um spherical droplets and created when both H_2O and H_2SO_4 vapors are saturated. Mixing ratio of H_2O vapor is fixed to be 30 ppmv below 30 km altitude and H_2SO_4 vapor is photochemically created around 62 km altitude. The resolution of the model is T42L120, and the calculation is conducted for 15 Earth years.

We found that the mixing ratio of H_2O vapor increases with latitude because it is mainly supplied from the lower atmosphere in the high latitude region. At the cloud level, the latitudinal distribution of H_2O vapor is almost determined by the residual mean meridional circulation, implying that the structure of the mean meridional circulation in the cloud layer can be investigated indirectly from the H_2O vapor distribution. H_2SO_4 vapor are photochemically created at 62 km altitude in the low latitude and transported toward the high latitude by the mean meridional circulation. And then, the clouds are mainly generated at 65 km altitude in the polar region and are the thickest in the high latitude region. This is qualitatively consistent with the previous infrared measurements conducted in the Pioneer Venus and Venus Express missions. The latitudinal distribution of H_2O vapor within the cloud layer is closely related to the residual mean meridional circulation.

金星には高度 50-70 km に分厚い硫酸の雲が広がり、全球的に金星を覆っている。赤外線や電波を用いた観測によって、金星の雲分布や雲の材料物質である水蒸気・硫酸蒸気混合比の分布は良く調べられている。しかし、この硫酸雲の生成・維持されるメカニズムについては良く分かっていない。本研究では、金星大気大循環モデル AFES-Venus に金星の雲物理過程を導入し、雲や雲材料物質の分布を決定する要因について理論的に調べた。

本研究では、過去の理論研究（Imamura & Hashimoto 1998; Hashimoto & Abe 2001）を参考にして以下のような仮定のもとで数値計算を行なった；雲材料物質として水蒸気と硫酸蒸気のみを考える。雲は硫酸の液滴で構成されており硫酸濃度は 85%に固定した。また、水蒸気と硫酸蒸気が両方とも飽和した時にのみ生成されるとする。雲の粒径として Mode1 と Mode2 のみを考え、それぞれの粒径を 0.5um と 1.0um に固定する。水蒸気は初期に高度 30km 以下に 30ppmv 存在しているとし、この混合比値は高度 30km 以下で一定とする。また硫酸蒸気は高度 62km 周辺で光化学的に生成されるとする。モデルの分解能は T42L120 であり、高度 0-120km の範囲で計算する。そして計算は 15 地球年行い、最後の 2 地球年のデータを主に解析した。

解析の結果、雲は極域で最も分厚くなることが分かり、Pioneer Venus や Venus Express の赤外観測と整合的である。水蒸気混合比は緯度共に大きくなり、Venus Express の VIRTIS の観測結果と定性的に整合する。硫酸蒸気混合比も高緯度で極大を持ち、Venus Express の電波掩蔽観測の結果と定性的に整合している。本発表では計算結果を示すと共に、雲や水蒸気・硫酸蒸気混合比分布を決定している物理過程について詳しく議論する。

ピリカ望遠鏡に搭載された近赤外エシェル分光器NICEよる金星大気微量分子の観測

築山 大輝 [1]; 前澤 裕之 [2]; 田中 培生 [3]; 高橋 英則 [3]; 大澤 健太郎 [3]; 高橋 幸弘 [4]; 佐藤 光輝 [5]; 今井 正尭 [6]; 大野 辰遼 [4]; 二村 有希 [4]; Lee Yeon Joo[7]
[1] 大府大・理・物理; [2] なし; [3] 東大・理・天文センター; [4] 北大・理・宇宙; [5] 北大・理; [6] 産総研; [7] JAXA/ISAS

Observation of minor constituents of Venusian atmosphere with NICE equipped on Pirka telescope

Daiki Tsukiyama[1]; Hiroyuki Maezawa[2]; Masuo Tanaka[3]; Hidenori Takahashi[3]; Kentaro Osawa[3]; Yukihiro Takahashi[4]; Mitsuteru SATO[5]; Masataka Imai[6]; Tatsuharu Ohno[4]; Yuki Futamura[4]; Yeon Joo Lee[7]
[1] Physical Science, Osaka Prefecture University; [2] none; [3] Institute of Astronomy, The University of Tokyo; [4] Cosmosciences, Hokkaido Univ.; [5] Hokkaido Univ.; [6] AIST; [7] JAXA/ISAS

We are carrying out the monitoring observations of atmospheres of the terrestrial planets in the solar system in order to understand the influences of activities of host stars on the atmosphere. In particular, Mars and Venus have already lost a magnetic field, therefore which are precious test sites suffering from the influence of the solar activities directly. We found that Venus had the short-term change in the mixing ratio of carbon monoxide in the middle atmosphere observed with a ground based millimeter wave band telescope, solar planetary atmosphere research telescope (SPART) placed in Nobeyama observatory (altitude 1350 m). This change is inexplicable by only influence of the solar activities. This indicates that the change is due to the complex circulations of materials in the Venusian atmosphere. The lower atmosphere below sulfuric acid clouds of Venus is difficult to observe by millimeter/submillimeter wave band heterodyne spectroscopies because of pressure broadening effects.

To address the short-term oxidation reaction networks and material circulations between lower and upper atmospheres on Venus, in July 2017 we demonstrated the scanning observation of absorption lines of CO, H_2O, SO_2, OCS with the slit of 2”x 7”and the wavelength resolution of 2,800 toward the night-side disk of Venus at K band by using Near-Infrared Cross-dispersed Echelle spectrograph, NICE equipped on Pirka telescope (Hokkaido Univ.) placed in Nayoro observatory (height 151 m). Although the atmospheric transparency was very low at the K band because of high humidity in Japanese rainy season and the observing condition at the low elevation (15-20 degrees), we succeeded in the detection of the absorption features of the above molecular species.This result suggests that NICE will enable us to carry out the spectroscopic monitoring of the atmospheres of the planets in the solar system at a site with good atmospheric transparency. At this stage NICE is planned to be installed on the 6.5 m optical-infrared telescope of the University of Tokyo Atacama Observatory (TAO) (alt. 5640 m) located on Cerro Chajnantor in the Atacama Desert of northern Chile.The wavelength coverage of NICE is 0.9-2.5 um (H, K, and I bands). This summer, we are planning to demonstrate test observations also in H band including the lines of hydrochloric acid.

中心星の活動が地球型の惑星の大気環境に与える影響について理解を深めるべく、我々は太陽系内惑星の大気の監視を推進している。特に火星や金星は磁場がなく、太陽活動の影響をダイレクトに受ける惑星大気の貴重な実験場である。金星においては、口径 10m のミリ波望遠鏡 SPART(国立天文台野辺山、標高 1350 m) での観測から、金星上層大気の一酸化炭素 (CO) の存在量が太陽活動の影響だけでは説明困難な短期的変動を有していることも分かってきた。こうした微量分子の変動は、金星大気の濃硫酸の雲より低高度の物質循環と連動していると考えられる。これらの高度はスペクトルが pressure broadening により広がるため、ミリ波帯のヘテロダイン分光では観測が難しい。そこで、我々は北海道名寄市立天文台 (標高 151 m) に設置された北海道大学所有の光赤外望遠鏡ピリカ (口径 1.6 m) に搭載された東京大学の近赤外中分散エシェル分光器 NICE(観測可能波長域 0.9-2.5 μ m) を用いて、下層大気の CO,H_2O,SO_2,OCS,HCl の吸収スペクトルの試験観測を実施した。これらの分子は金星大気の酸化反応ネットワークにおいて重要な役割を果たす。観測は 2017 年の 7 月に実施し、観測波長は K バンド、波長分解能 2800(2” スリット) の高分散分光で、金星の視直径 16” に対し、2” × 7” のスリットで夜面をスキャン/積分を行った。夏季であり EL も 15-20 度と低く厳しい観測条件ではあったが、金星や地球の大気の近赤外域の放射輸送モデルとの詳細な比較検証を実施し、NICE による初めての系内惑星の大気分子の吸収スペクトル線の検出に成功した。この結果は、大気透過度の高いサイトでの NICE の惑星大気観測へのポテンシャルを示すものであり、今夏、H バンドでも金星大気の高分散分光観測を計画している。その後、NICE はアタカマ高地 (標高 5640 m) の東京大学アタカマ天文台 (TAO)(口径 6.5 m) に搭載される予定である。

Identification of a UV absorber in the Venus atmosphere by FUJIN

Yukiko Shirafuji[1]; Makoto Taguchi[2]; Masataka Imai[3]; Yukihiro Takahashi[4]; Mitsuteru SATO[5]; Toshihiko Nakano[6]; Yasuhiro Shoji[7]
[1] Physics, Rikkyo Univ.; [2] Rikkyo Univ.; [3] AIST; [4] Cosmosciences, Hokkaido Univ.; [5] Hokkaido Univ.; [6] Space Engineering, Tohoku Univ.; [7] JAXA

Ground-based optical telescopes have been used for astronomical observations, however, they have the following problems. Absorption by the ozone layer makes it impossible to observe wavelengths shorter than 300 nm. A continuous observation of an celestial object for a long period is difficult, unless multiple observatories with equal performance and longitudinal separation are available. Optical seeing is a measure of deterioration of spatial resolution due to atmospheric fluctuation, and spatial resolution for a ground-based observation usually cannot reach the diffraction limit. Therefore, observations from space platforms such as airplanes, artificial satellites and balloons have been developed. Satellite telescopes are free from influence by the earth's atmosphere. However, they are quite expensive, and in-orbit service for maintenance is almost impossible. A balloon-borne telescope has been proposed to overcome such disadvantages of the ground-based and satellite observations.

FUJIN-2 is a project to study phenomena in the planetary atmospheres and plasmas by an optical telescope suspended by a balloon up to the polar stratosphere at an altitude around 32 km. FUJIN-2 can observe planets for a long continuous period in a wide wavelength range without the seeing problem. Seeing is expected to be 0.1"" or less at that altitude, smaller than the diffraction limited spatial resolution of a visible telescope with an aperture of 1 m. Since FUJIN-2 floats above the peak density of the ozone layer, it is possible to observe wavelengths of 280 nm by FUJIN-2. Planets can be continuously observed for a long period especially from the polar stratosphere. On the other hands the balloon-borne telescope has a disadvantage that its launch depends on the weather condition. We regard that the above merits of the balloon-borne telescope surpass those of the other observation platforms even the disadvantage of balloon observation is admitted.

Venus is covered with thick sulfuric acid ($H_{-}\{2\}SO_{-}\{4\}$) clouds throughout the altitude range of 45-70 km. The cloud layer, not the ground surface, absorbs solar radiation and heats the atmosphere. At an altitude of 64 km, 50% of the solar radiation is scattered and absorbed [Tomasko et al., 1980]. The Venus atmosphere also has a special general circulation called as a super rotation, which circulates the entire planet to the west. The wind speed of the super rotation reaches 100 m/s at an altitude of 70 km, 60 times faster than the rotation speed of the solid body.

Attempts to reproduce the high velocity wind by numerical models are indispensable approaches to theoretically explain the super rotation, and so far a large number of studies have been carried out. However, understanding about the solar heating is insufficient, making it difficult to build a sophisticated model which reflects the realistic solar heating and distributions of chemical species. The main reason for this is that an absorber of a broad absorption band in the wavelength range of 320 - 500 nm is still unidentified. The ultraviolet absorption band for the wavelength region shorter than 320 nm is well explained by absorption due to $SO_{-}\{2\}$ centered at 283 nm. However, the absorption in the wavelength region longer than 320 nm cannot be explained by SO_2. Absorbing materials containing S (sulfur) have been proposed to explain the absorption in these several decades. Recently, it is shown that S_2O or OSSO are the most promising candidates for reproducing the edge of the absorption band at 400 - 500 nm. However, because the wavelength resolution of the spectral observation in the past was about 4 nm, the characteristic absorption structures of S_2O and OSSO could not be resolved. Therefore, observation by a spectrometer with a wavelength resolution higher than 0.4 nm is proposed for the main target of FUJIN-2. A test spectroscopic observation of Venus from the ground has been prepared, and the results will be presented.

火星探査機MRO搭載熱赤外センサMCSで観測された気温・ダスト・水氷雲の相関

上田 真由 [1]; 野口 克行 [1]; 林 寛生 [2]
[1] 奈良女大・理・環境; [2] 富士通 FIP

Zonal correlation among dust, water ice clouds and temperature in the Marian atmosphere observed by MRO-MCS

Mayu Ueda[1]; Katsuyuki Noguchi[1]; Hiroo Hayashi[2]
[1] Nara Women's Univ.; [2] Fujitsu FIP

Mars is the fourth planet from the Sun and its climate is colder than Earth. Water ice clouds and dust floating in the atmosphere play an important role to determine the temperature distribution in the Martian atmosphere. We studied the relationship among dust opacity, water ice cloud opacity and air temperature observed by Mars Climate Sounder (MCS) onboard Mars Reconnaissance Orbiter (MRO). Our previous analysis showed that dust opacity and temperature around 30-60S (Hellas Planitia) increased and water ice cloud opacity in the same region decreased simultaneously. We studied the zonal correlation among them and found a positive correlation between dust and temperature, a negative correlation between temperature and water ice clouds and a negative correlation between water ice clouds and dust. On the other hand, we have found a strong positive correlation between dust and water ice clouds in a more northern region (30S-equator). We further studied the relationship between each physical quantity and its correlation coefficient.

火星は地球の外側に位置する第4惑星であり、地球に比べて寒冷な惑星である。火星の気温分布を決める要因として、水氷雲と大気中に浮遊する砂埃(ダスト)が挙げられる。本研究では、気温、ダスト、水氷雲の相関を明らかにすることを目的とする。これまでの研究では、米国の火星探査機Mars Reconnaissance Orbiter（MRO）搭載のMars Climate Sounder（MCS）で得られたデータによって、南緯30度～60度付近(ヘラス盆地)の上空でダストが増加すると共に気温も上昇し、水氷雲が減少すると言う関係が見つかっていた。そこで、これら3変数の東西方向の分布に対して相関係数を求めたところ、ダストと気温には正の相関、水氷雲と気温には負の相関、ダストと水氷雲には負の相関が見られた。一方、ヘラス盆地よりも北側(南緯30度～赤道付近)では、ダストと水氷雲に強い正の相関が見られた。なぜこのような違いが現れるのかを説明する手がかりとするために、さらに各物理量の絶対値と相関係数の関係を解析した。

火星のO2分布と化学：テラヘルツセンサによる観測を見据えて

黒田 剛史 [1]; 山田 崇貴 [2]; Larsson Richard[1]; 佐川 英夫 [3]; 青木 翔平 [4]; 笠井 康子 [1]; 前澤 裕之 [5]; 笠羽 康正 [6]
[1] NICT; [2] 東工大・総理工・化環; [3] 京都産業大学; [4] BIRA-IASB; [5] なし; [6] 東北大・理

O2 distributions and related chemistry on Mars: Towards the investigations with the future Mars terahertz sensor missions

Takeshi Kuroda[1]; Takayoshi Yamada[2]; Richard Larsson[1]; Hideo Sagawa[3]; Shohei Aoki[4]; Yasuko Kasai[1]; Hiroyuki Maezawa[5]; Yasumasa Kasaba[6]
[1] NICT; [2] Tokyo Tech; [3] Kyoto Sangyo University; [4] BIRA-IASB; [5] none; [6] Tohoku Univ.

The importance of O_2 (molecular oxygen) for the atmospheric chemistry on Mars had been overlooked historically, because it has been thought to exist horizontally and vertically constant (~1400 ppmv) and impossible to observe from ground-based telescopes due to the deep absorption of the terrestrial O_2. However, the recent sub-millimeter spectroscopic observation using the Herschel Space Observatory suggested the possibility of higher concentration of O_2 near the Martian surface based on which detected the non-uniform vertical distribution of O_2 in global-mean abundance [Hartogh et al., 2010], and, since then, we have started to investigate the importance of O_2 for the atmospheric environment of Mars.

The abundance of O_2 is chemically related to the existences of O_3, H_2O, HO_2, H_2O_2, CO and methane. Simulated results by a Mars global climate model (MGCM) including a chemical suite (Mars Climate Database v5.3) did not show the specific vertical variances of O_2 abundance except the winter polar regions where the composition changes due to the condensation of CO_2. It means that current MGCMs may lack the processes which cause the vertical gradient in the O_2 abundance that suggested by the Herschel observation: e.g., unusual chemical reactions inside local dust storms and/or other surface activities including biological and geological ones.

Terahertz sensors which are planned to be onboard future satellite missions may observe the abundances of O_2 and chemically-related molecules (O_3, H_2O, H_2O_2), and would be suitable for the first specific observational investigations of O_2 distributions and its formation/loss processes on Mars. In this presentation we show test experiments of O_2 distributions using our MGCM (DRAMATIC) with water cycle and a preliminary chemical module, and discuss the potential scientific interests for future terahertz observations from Mars landers/orbiters.

Mars mesospheric zonal wind at global dust storm 2018

Hiromu Nakagawa[1]; Shohei Aoki[2]; Takeshi Kuroda[3]; Hideo Sagawa[4]; Naoki Terada[5]; Yasumasa Kasaba[6]; Kosuke Takami[1]; Nao Yoshida[7]; Katsushige Toriumi[8]; Akiho Miyamoto[1]
[1] Geophysics, Tohoku Univ.; [2] BIRA-IASB; [3] NICT; [4] Kyoto Sangyo University; [5] Dept. Geophys., Grad. Sch. Sci., Tohoku Univ.; [6] Tohoku Univ.; [7] Geophysics, Tohoku Univ.; [8] Geophysics, Tohoku Univ

The temperature and density profiles observed in the middle to upper atmospheres on Mars show substantial perturbations resulting from superposition of various atmospheric waves, including the gravity waves (GWs). GWs are known to play an important role in determining the general circulation in the middle atmosphere by dynamical stresses caused by GW breaking. Recent MAVEN also revealed that the observed wavelike perturbations in the upper atmosphere likely represent upward propagating GWs of tropospheric origin (Nakagawa et al., under revision). Numerical simulations demonstrated that the filtering effect by background winds plays a major role in the vertical propagation of GWs generated in the lower atmosphere. The processes and dynamics in the middle atmosphere have thus an important role on the regional coupling between lower and upper atmosphere. Yet, very few direct measurements have been performed so far, and the general circulation in the middle atmosphere on Mars relies on General Circulation Models (GCMs). Recent studies have highlighted the efficiency of mass transport from the lower to upper atmospheric reservoir and increase of the atmospheric water loss in the southern summer, which happens to be a dusty season (at a solar longitude, Ls, of 240 degree or later). Answering questions about the atmospheric coupling between lower and upper atmosphere and their links with dust activities in the troposphere is a key to an understanding the mechanisms of the mass transport into the upper atmosphere.

Sonnabend et al. (2002) reported zonal wind measurements at about 80 km altitude around northern spring equinox, by using mid-IR wavelengths heterodyne technique which provides 10-100 times improved spatial resolution over sub-mm or radio observations. They showed highly variable nature of the winds in the range between 180 m/s prograde to -94 m/s retrograde. At present, the source to drive the variability has yet to be fully quantified. Currently, a very strong dust storm has developed on Mars for the first time after the previous one occurred in 2007. This is a rare opportunity to observe drastic changes in the Martian atmosphere under such a strong dust storm. Here we present direct observations of Mars zonal wind velocities around northern fall equinox to northern winter during Mars Year (MY) 34 global dust storm.

Observations were carried out using Mid-Infrared Laser Heterodyne Instrument (MILAHI) at the Tohoku-0.6m dedicated telescope Facility on Haleakala, Hawaii for continuous monitoring. A detailed description of the instrument is given by Nakagawa et al. (2016). On 27 June 2018 (Ls = 200 deg), we observed Mars whose angular diameter to be ˜20.6 arcsec against the diffraction-limited field of view (FOV) of the telescope of ˜4.3 arcsec. The acquisition time for an individual spectrum was ˜5 min. Spectra were co-added to achieve a sufficient signal-to-noise ratio. The instrument beam has been switched during observing run between limb-geometry at the equatorial dayside limb and nadir-geometry at the martian disk center, in order to extract the zonal wind-doppler effect. The retrieved wind velocities was found to be -48〜-56 m/s, which is basically in an agreement with previous study. To assess implications of the observations, we will perform simulations with a high-resolution MGCM which captures life cycles of a significant portion of small-scale GWs including generation, propagation, and dissipation.

This massive dust storm could engulf Mars for months. We will be continuing to monitor the middle atmosphere. The next campaign will be performed during 22 August and 6 September 2018 (Ls = 240 deg), while the dust continues to slowly settle out of the atmosphere. In this paper we will also introduce the coordinated observations by ALMA. Our ToO observations have been successfully performed on 30 June and 16 July 2018.

Effects of the IMF direction on Martian atmospheric escape under a weak intrinsic magnetic field

Shotaro Sakai[1]; Kanako Seki[1]; Naoki Terada[2]; Hiroyuki Shinagawa[3]; Ryoya Sakata[1]; Takashi Tanaka[4]; Yusuke Ebihara[5]
[1] Dept. Earth & Planetary Sci., Science, Univ. Tokyo; [2] Dept. Geophys., Grad. Sch. Sci., Tohoku Univ.; [3] NICT; [4] REPPU code Institute; [5] RISH, Kyoto Univ.

Understanding the atmospheric escape mechanism leads to reveal the Martian climate history. Present Mars has a thin atmosphere and little water on the surface, while ancient Mars could keep liquid water and a thick atmosphere. This suggests that Mars has experienced significant atmospheric loss from the past through the present. The atmosphere escapes as shapes of neutral gas or ions. Ion outflow is one of the important atmospheric loss mechanisms. In the present day, Mars does not have a global magnetic field such as that of Earth, and thus, ions escape by the direct interaction with the solar wind. In contrast, it is expected that ancient Mars had a global magnetic field. The global magnetic field forms the magnetosphere around the planet and change the ion escape mechanism. Sakai et al. (2018) showed that the existence of a weak dipole field results in an enhancement of the ion escape rate under a parker spiral type interplanetary magnetic field (IMF).

In this study, effects of the IMF direction on the ion escape processes under the intrinsic magnetic field of 100 nT at the equatorial surface are investigated based on global multispecies single-fluid magnetohydrodynamics simulations (Terada et al., 2009; Sakai et al., 2018). Ion escape processes from Mars under two IMF conditions, namely, a northward and a parker-spiral cases, are compared. In the parker-spiral case, heavy ions escape through the two channels associated with the open field lines and other two channels associated with a magnetic reconnection between the planetary and solar wind magnetic fields at the flank magnetopause (Sakai et al., 2018). In contrast, the heavy ions mainly escape through the open field line related to the cusp in the northward case. The escape rate of heavy ions in the north-IMF case is about one order of magnitude smaller than in the parker-spiral IMF case and it is even smaller than in the no-dipole case. It suggests that the interaction of the weak intrinsic magnetic field and northward IMF forms the firm magnetosphere, resulting in suppressing the ion escape. The results also show that the IMF direction significantly affects the ion escape processes.

References:

Sakai, S., Seki, K., Terada, N., Shinagawa, H., Tanaka, T., & Ebihara, Y. (2018). Effects of a weak intrinsic magnetic field on atmospheric escape from Mars. Geophys. Res. Lett., submitted.

Terada, N., Kulikov, Y. N., Lammer, H., Lichtenegger, H. I. M., Tanaka, T., Shinagawa, H., & Zhang, T. (2009). Atmospheric and water loss from early Mars under extreme solar wind and extreme ultraviolet conditions. Astrobiology, 9, 55-70. https://doi.org/10.1089/ast.2008.0250

Energy dependence of elastic collisions between magnetospheric electrons and neutral H2O molecules in the Enceladus torus

Hiroyasu Tadokoro[1]; Yuto Katoh[2]
[1] Musashino University; [2] Dept. Geophys., Grad. Sch. Sci., Tohoku Univ.

Water group neutrals (H_2O, OH, and O) in Saturn's inner magnetosphere play the dominant role in loss of energetic electrons and ions because of abundance of the neutrals [e.g., Paranicas et al., 2007,2008; Sittler et al., 2008]. Previous studies suggested that the neutral cloud originated from Enceladus contributes to loss processes of plasma in the magnetosphere. However, little has been reported on a quantitative study of the electron loss process due to electron-neutral collisions. Conducting one dimensional test-particle simulation, Tadokoro et al. [2014] examined the time variations of equatorial pitch angle distribution and electrons within loss cone through 1 keV electron pitch angle scattering due to electron-H_2O elastic collisions around Enceladus when the electron flux tube passes the region of the dense H_2O molecules in the vicinity of Enceladus (˜380 sec). The result showed that the electrons of 11.4 % are lost in ˜380 sec. The estimated loss rate was twice faster than the loss time under strong diffusion. Assuming the uniform azimuth H_2O density structure in the torus, they also estimated the electron loss rate of 33 % during one corotation. Next remaining issue is a calculation of energy dependent electron loss rate. We show the loss rate of electrons with 500eV-50keV and the comparison of the loss rate between the high (in the vicinity of Enceladus) and low (in the Enceladus torus) H_2O density regions. We also show energy dependent loss rate with error bars by conducting the calculation several times.

Variation of heavy ions' precipitation on the Mercury's surface

Manabu Yagi[1]; Kanako Seki[2]; Yosuke Matsumoto[3]; Dominique Delcourt[4]; Francois Leblanc[5]
[1] RIKEN R-CCS; [2] Dept. Earth & Planetary Sci., Science, Univ. Tokyo; [3] Chiba University; [4] LPP, Ecole Polytechnique, CNRS; [5] LATMOS-IPSL, CNRS

Observations by MESSENGER found that Mercury's magnetosphere is analogous to the Earth's while there are several differences of the two. One of the big differences is a dipole offset which could affect to the global configuration of Mercury's magnetosphere especially making a strong north-south asymmetry. In this study, first we performed many cases of MHD simulation solving an interaction with solar wind plasma and offset dipole of Mercury. Solar wind densities are given betwenn nominal(35cm^{-3}) and high(140cm^{-3}) with velocities for 400km/s to 800km/s, which are almost average value in the Mercury's orbit. An important parameter which could change the global structure of magnetosphere is IMF condition. IMF conditions are comes from Parker's spiral which has strong Bx component at the Mercury's orbit in addition to the ideal one which has only Bz component for comparison.

When solar wind density is nominal, the structure of Mercury's magnetosphere is not far from miniature of Earth's magnetosphere, while north-south asymmetry is outstanding because of the offset dipole. In the realistic IMF case, global configurations of magnetosphere drastically change and become more complicated structures which include stronger north-south and dawn-dusk asymmetry by strong Bx and weak By components. IMF Bx also affects to the intensity ratio of north and south cusp pressure, and By component twist the cusp region to longitudinal direction. The heavy ions' trajectories basically obey the global structure of magnetic field, so that the ions' precipitation concentrate on the "magnetic cusp" defined from MHD simulations, but the precipitation region is wider and the boundary is not clear compared to the MHD cusp. In the presentation, we will discuss more details of heavy ion precipitation pattern. The identification of global structures and ions' precipitation region especially the cusp is important not only on the understanding of magnetospheric physics itself, but also making a proposal to the observational plan of spacecraft such as Bepi-Colombo.

荷電粒子照射による宇宙風化再現実験で明らかにする氷衛星の内部進化

木村 智樹 [1]; 木村 淳 [2]; 吉岡 和夫 [3]; 村上 豪 [4]
[1] Tohoku University; [2] 阪大・理・宇宙地球; [3] 東大・新領域; [4] ISAS/JAXA

Evolution of Icy Moon’s Interior Uncovered by Laboratory Experiment: Modeling of Space Weathering by Ion Irradiation

Tomoki Kimura[1]; Jun Kimura[2]; Kazuo Yoshioka[3]; Go Murakami[4]
[1] Tohoku University; [2] Earth & Space Science, Osaka Univ.; [3] The Univ. of Tokyo; [4] ISAS/JAXA

In our solar system, several icy bodies have liquid water ocean underneath solid surface, while only Earth has ocean on the surface. The subsurface ocean is potentially universal habitable environment. Differentiation of the icy body’s interior is an unsolved big problem for the subsurface ocean and also for the possible life that has likely been evolving there. We try to pin down the differentiation process based on the space weathering on the icy body’s surface that is driven by irradiation of space plasma. In this study, long-term space weathering at Ganymede that reaches Giga years is modeled by ion irradiation to the possible surface material, epsomite, with laboratory beam experiment. Chronology for Ganymede’s surface material is made based on the altered spectrum of surface material. Dependence of surface material age on the intrinsic magnetic field strength of Ganymede is investigated based on comparison of our laboratory experiment with the surface spectroscopy by the Galileo explorer. We discuss the age of Ganymede’s magnetic field and the differentiation process of molten interior that drives the magnetic field. In this presentation, we report current status of our laboratory experiment made with an ion injector at the Wakasa-wan Energy Research Center.

In our solar system, several icy bodies have liquid water ocean underneath solid surface, while only Earth has ocean on the surface. The subsurface ocean is potentially universal habitable environment. Differentiation of the icy body’s interior is an unsolved big problem for the subsurface ocean and also for the possible life that has likely been evolving there. We try to pin down the differentiation process based on the space weathering on the icy body’s surface that is driven by irradiation of space plasma. In this study, long-term space weathering at Ganymede that reaches Giga years is modeled by ion irradiation to the possible surface material, epsomite, with laboratory beam experiment. Chronology for Ganymede’s surface material is made based on the altered spectrum of surface material. Dependence of surface material age on the intrinsic magnetic field strength of Ganymede is investigated based on comparison of our laboratory experiment with the surface spectroscopy by the Galileo explorer. We discuss the age of Ganymede’s magnetic field and the differentiation process of molten interior that drives the magnetic field. In this presentation, we report current status of our laboratory experiment made with an ion injector at the Wakasa-wan Energy Research Center.

ALMAアーカイブデータ解析によるイオ大気中の火山起源分子の空間分布

鈴木 達也 [1]; 平原 靖大 [2]; 古賀 亮一 [3]; 坂野井 健 [4]; 菅原 徹也 [5]
[1] 名大・環; [2] 名大・院・環境・地球惑星; [3] 東北大・理・地物; [4] 東北大・理; [5] 名大・環

Spatial Distributions of Molecules originated from volcanoes on Io by analysis of ALMA archive data

Tatsuya Suzuki[1]; Yasuhiro Hirahara[2]; Ryoichi Koga[3]; Takeshi Sakanoi[4]; Tetsuya Sugawara[5]
[1] Earth Sciences, Nagoya Univ.; [2] Earth&Planetary Sciences, Nagoya Univ.; [3] Geophysics, Tohoku Univ.; [4] Grad. School of Science, Tohoku Univ.; [5] Environmental studies, Nagoya Univ.

On the Io's surface, volcanic activity occurs frequently. The gases of volcanic plume condensate as frost and covers around the surface. Sublimation of frost and outgassing from volcanic plume support Io's atmosphere which requires a continuous replenishment. However, the relative contributions of the different sources is still poorly understood. According to some previous papers, sublimation of frost dominates the support of Io's atmosphere [e.g., Tsang et al., 2016]. In (sub)millimeter region, spectral lines of SO2 were obtained at IRAM-30 m antenna [Lellouch, 1996] and lines of SO_2, SO and NaCl were observed by SMA [Moullet et al., 2010]. Recently, the observation by ALMA, which is the interferometer consisted of 54 12m-arrays and 12 7m-arrays, were executed [e.g., Moullet et al., 2014].

The goal of our research is a discussion for spatial distributions of atmospheric molecules and temperature on Io with the observation data of ALMA. The archive data of observations executed in 2012, 2013 and 2016 are accessible. In the observations, ALMA observed SO_2, SO, NaCl, KCl emission lines at 250˜350GHz. The angular resolution of them were less than 0.8 arcsec, which is less than one tenth as large as the apparent size of Io. For detailed quantitative analysis for the Io's atmosphere, radiative transfer modeling in non-local thermal equilibrium is required because of the very diffuse condition (few nano bar). In this conference, we present the fitting result of modeling for the observation in 2016 (project code: 2015.1.00995.S) and the assumption for models. This observation was executed while Io's escaping from Jovian shade. Thus, the atmosphere's response to sunlight will be analyzed from this data and we can calculate the contribution of sublimation.

木星の衛星イオに全球的に存在する火山からの噴出物は霜として火山周辺に堆積している。イオの数 nbar の大気の構成分子は SO_2 を主として、SO、NaCl、KCl、Na などがあり、火山からの直接の噴出物のほか、堆積した霜の昇華によって持続的に供給されていると考えられる。供給源それぞれの相対的な寄与度はよくわかっていない。先行研究では、紫外領域や赤外領域でのスペクトル観測によって、大気の不均質な分布や個々の供給源などが議論されてきた [e.g. Spencer et al., 2005; Geissler et al., 2007; Tsang et al, 2016]。それらでは、火山活動にも依るが、霜の昇華が大気供給を支配していることが示唆されている。(サブ) ミリ領域での観測では、IRAM での SO_2 輝線の観測 [Lellouch, 1996] や SMA での SO や NaCl を含めた大気の観測 [Moullet et al., 2010] が行われており、近年では ALMA(アタカマ大型ミリ波サブミリ波干渉計) を用いた観測 [e.g. Moullet et al., 2014] も行われている。

本研究は、ALMA による観測データを用いて、大気物質の分布と励起温度を高精度で導出することを目指す。ALMA の高い周波数分解能と高感度な観測によって、SO や NaCl といった微量分子も観測が可能である。現在までに、2012 年、2013 年、2016 年のアーカイブ観測データのデータリダクションを終了し、高次解析を進めている。2016 年の観測は木星の影から脱出する前後のイオ大気の観測であり、脱出開始の 60 分後から 100 分の間にディスク平均の輝度温度が 68K から 82K (262.2GHz) に回復していることが分かった。これは、太陽光によるイオの霜の昇華過程の応答時間と SO_2 の大気への供給の寄与度を示している。

解析データをより定量的に解釈する上で、で得られたイオの非-局所的熱平衡状態での放射伝達モデリングが必要で、現在プログラムの開発を進めている。ここでは、2016 年の観測における解析結果を示す。

すばる望遠鏡で観測された木星赤外オーロラの微細構造とその時間変動

渡辺 はるな [1]; 北 元 [2]; 垰 千尋 [3]; 鍵谷 将人 [4]; 坂野井 健 [5]; 笠羽 康正 [6]
[1] 東北大・理・地球物理; [2] 東北大・理・惑星プラズマ大気; [3] 情報通信研究機構; [4] 東北大・理・惑星プラズマ大気研究センター; [5] 東北大・理; [6] 東北大・理

Fine structures of Jovian infrared auroras and their time variations obtained with the Subaru IRCS

Haruna Watanabe[1]; Hajime Kita[2]; Chihiro Tao[3]; Masato Kagitani[4]; Takeshi Sakanoi[5]; Yasumasa Kasaba[6]
[1] Geophysics, Tohoku Univ.; [2] Tohoku Univ.; [3] NICT; [4] PPARC, Tohoku Univ; [5] Grad. School of Science, Tohoku Univ.; [6] Tohoku Univ.

Jovian Infrared aurora is an emission of H_3^+ produced by electron precipitation and ion chemistry and thermalized by H_2 atmosphere. Its morphology and intensity have been studied by observations using ground-based telescopes and space probes. In the past ground-based infrared observation, the best temporal resolution was ~16 min and the spatial resolution was ~1 arcsec. The fastest time variation reported was seen in the polar emission with ~30 min [Stallard et al., 2016]. On the other hand, Hubble space telescope data showed that the ultraviolet aurora, which is considered to directly reflect electron precipitation, has a faster time variation on a time scale of 2-11 min.

We observed Jovian H_3^+ infrared aurora with the Infrared Camera and Spectrograph (IRCS) attached on the Subaru telescope at Mauna Kea, Hawaii. We used an H3P narrow-band filter (central wavelength: 3.413 um), which covers four strong H_3^+ emission lines. The observation was performed on 31 January 2015 (8:38-15:36 UT) and 25 May 2016 (6:53-7:46 UT). We got the slit views with spectrograph mode at the former observation, and used imaging mode at the latter observation. The adaptive optics instrument (AO188) enabled us to obtain high spatial resolution (~0.2 arcsec) images.

From the data obtained in 2016, patch-like emissions were seen on the noon sector of the northern polar region and they pulsated on a time scale of ~10 min. Considering that temperature change occurs over the timescale of $>$~10^3-10^4 s/K, transport and diffusion occurs over the timescales of 10^4-10^5 s, the pulsating intensity variation is likely to be caused by H_3^+ density change by electron precipitation. We utilized the auroral emission model to investigate the dependence of H_3^+ emission decay time to the energy of precipitating electron. It was revealed that the fastest decay (~10 min) of auroral emission is made by the electron with the energy range from ten to a few tens of keV, while lower or higher energy electrons make slower decay. Next, we evaluated the response of the H_3^+ emission intensity to the periodic electron flux variation over the various time scales. We confirmed that the H_3^+ emission intensity with the time scale of ten to a few tens of minutes could be caused by the modulation of the auroral electron flux variation with similar time scales.

In this presentation, we focus on the results of the observation on 31 January 2015. We observed the southern aurora during 8:38-8:47 (UT), and observed the northern aurora during 9:49-10:45 and 11:45-13:41 (UT). In one observation run, we get several images of Jupiter, several images of sky, and then get several images of Jupiter again. Four sets were performed for the southern aurora and nine sets were performed for the northern aurora. The interval of the successive images was ~40 sec, and the interval of each set was ~4 min. We summarize the characteristics of auroral structures as follows:

(1) On the northern main emission, the sector in the westward of ~200 deg. system III (SIII) was bright, and that in the the ~160-190 deg. SIII longitude was faint. Some bright filamentary structures were seen in the dusk sector.

(2) On the ~300-340 deg. SIII longitude of the southern main oval, auroral emission was faint. Some patch-like structures were seen in this sector.

(3) Southern Io's footprint extended surrounding the main emission. For example, when the Io's footprint spot was at the SIII longitude of ~320 deg., the end of the tail was at ~270 deg. On the other hand, the northern footprint was not so long.

(4) Some patch-like or filamentary emissions were seen in the noon sector of the northern polar region. There was no periodic pulsating structure like 2016 observation data.

We will present the comparison of observation data taken in 2015 and 2016, and their spatial and temporal characteristics.

木星 H_3^+ オーロラは磁気圏または太陽風からの電子の降りこみによって電離圏中に H_3^+ イオンが生成され、それが H_2 大気中で熱的に励起されて起こる発光である。その形状や強度は地上大型望遠鏡や探査機による観測から明らかにされてきた。過去の地上望遠鏡赤外観測における最高の時間分解能は約 16 分、空間分解能は約 1 秒角であり、極域発光構造の 30 分変動が報告された [Stallard et al., 2016]。一方、電子の降りこみを直接的に反映していると考えられる紫外オーロラは、ハッブル宇宙望遠鏡により 2-11 分スケールの変化が観測されている。

我々はハワイ・マウナケア山頂のすばる望遠鏡赤外分光撮像装置（IRCS）の H3P narrow-band filter（中心波長 3.413 um、H_3^+ イオンの主要な輝線を含む）を用いて、木星赤外オーロラの撮像を行った。観測は 2015 年 1 月 31 日（8:38-15:36

UT）と 2016 年 5 月 25 日（6:53-7:46 UT）の 2 回行った。前者は分光モードでスリット画像を取得し、後者は撮像モードで観測を行った。補償光学装置 AO188 を用いることにより、これまでの地上観測よりも高い空間分解能（約 0.2 秒角）を実現することができた。

2016 年 5 月 25 日の観測では、北側極域昼側に複数のパッチ状発光が見られた。それらのパッチ状構造は、約 10 分の周期で明滅していた。熱圏の温度変化や H_3^+ イオンの輸送の時定数は 10^4-10^5 秒 [Tao et al., 2013] と長いことから、観測された発光強度変動はオーロラ電子の降りこみによる H_3^+ 密度の変化を反映している事が示唆される。我々はオーロラ発光モデル [Tao et al., 2011] を用いて、赤外オーロラの発光強度減衰にかかる時間の、降りこみ電子のエネルギーへの依存性を調べた。その結果、10 keV から数十 keV の降りこみ電子が引き起こすオーロラ発光の減衰が最も早く 10 分間程度であり、、それより低エネルギーまたは高エネルギーになるにつれて減衰が遅くなることが分かった。次に、降りこみ電子のフラックスを様々な周期で変動させた結果、10 分から数十分の電子フラックス変動は同程度の周期のオーロラ発光強度変動を引き起こすことが分かった。

本発表では主に、2015 年 1 月 31 日の観測結果について報告する。この観測では 8:38-8:47 (UT) に南オーロラの撮像を行い、9:49-10:45 および 11:45-13:41 (UT) に北オーロラの撮像を行った。木星を数枚撮像し、スカイを数枚撮像、そして再び木星を数枚撮像するという一連の作業を 1 セットとし、南オーロラに対して 1 セット、北オーロラに対して 9 セット行った。連続して撮像した木星イメージ同士の間隔は約 40 秒、1 セットと 1 セットの間隔は約 4 分であった。解析結果から、次のような特徴が見られた。

(1) 北側メインオーバルは System III (SIII) 経度˜200 度以西が明るく、˜160-190 度が暗かった。また dusk 側には明るいフィラメント状の構造が複数並んでいた。

(2) 南側メインオーバルは SIII 経度˜300-340 度が暗く、その経度範囲ではメインオーバル上にパッチ状構造が見られた。

(3) 南側のイオフットプリントがメインオーバルを囲むように長く伸びていた。スポットが SIII 経度約 320 度にあるとき、尾の終わりが約 270 度まで伸びていた。一方北側のイオフットプリントはそのように長く伸びてはいなかった。

(4) 北側極域昼側にパッチ状およびフィラメント状の発光構造が見られた。2016 年の観測でみられたような周期的な明滅は見られなかった。

発表では、2015 年と 2016 年の観測結果を比較し、形状や発光強度、時間変動について報告する。

Expected source region of Jupiter's hectometric radio component relating to magnetotail reconnection

Hiroaki Misawa[1]; Fuminori Tsuchiya[2]; Takahiro Mizuguchi[2]
[1] PPARC, Tohoku Univ.; [2] Planet. Plasma Atmos. Res. Cent., Tohoku Univ.

It has been known that Jupiter's auroral radio emission in the hectometric wave range (HOM) is roughly classified two type occurrence components. One is a component relating to solar wind variations (sw-HOM) appearing around CML(Central Meridian system III Longitude of an observer) ˜180deg when solar wind pressure enhances. The other one is generally more intense than sw-HOM and has no or weak relation with solar wind variations (nsw-HOM) appearing around CML ˜110deg and ˜280deg for major components when De (Jovicentric declination of an observer) ˜-1deg (Nakagawa et al., 2000; Nakagawa, 2003). Recently, we found one more nsw-HOM component appearing around CML ˜340deg, which highly correlates occurrence of magnetic reconnection events in the magnetotail region based on the WIND/WAVES data analyses (Misawa et al., 2018). This new component is an important role for the studies of global magnetospheric dynamics of Jupiter since it is a possible remote marker of the reconnection events occurring in the magnetotail. However, due to difficulty in precise direction finding in the hectometric wave range, the radio source of the new component, that is, location of transported energy input originated from reconnection events, has been still unrevealed.

In order to investigate source location of the new nsw-HOM we have made a comparison study of the new component with appearance features of Jupiter's aurora observed by the Hubble Space Telescope (HST) and the Hisaki spacecraft, and also have surveyed expected source regions by calculating observable rays using a magnetic field model. Preliminary analyses show that the occurrence of the new component well correlate with intensification of Jupiter's internally driven type aurora, and expected radio sources are located around dawn (spot) region and/or polar region.

Acknowledgements: We would greatly appreciate M. Kaiser, J.-L. Bougeret and the WIND/WAVES team for providing the radio wave data, and J. T. Clarke and C. Tao for providing Jupiter's aurora data.

電子反射法を用いた太陽風中での月面磁場強度推定

＃川口 友暉 [1]; 原田 裕己 [2]; 斎藤 義文 [3]; 横田 勝一郎 [4]; 西野 真木 [5]; 臼井 英之 [6]; 三宅 洋平 [7]; 加藤 大羽 [8]; 綱川 秀夫 [9]
[1] 京大・理・地惑; [2] 京大・理・地球惑星; [3] 宇宙研; [4] 阪大; [5] 名大 ISEE; [6] 神戸大・システム情報; [7] 神戸大学; [8] 東大・理・地惑; [9] 東工大・理・地惑

Lunar surface magnetic field intensity in the solar wind inferred from electron reflectometry

Tomoki Kawaguchi[1]; Yuki Harada[2]; Yoshifumi Saito[3]; Shoichiro Yokota[4]; Masaki N Nishino[5]; Hideyuki Usui[6]; Yohei Miyake[7]; Daiba Kato[8]; Hideo Tsunakawa[9]
[1] Geophysics, Kyoto Univ.; [2] Dept. of Geophys., Kyoto Univ.; [3] ISAS; [4] Osaka Univ.; [5] ISEE, Nagoya University; [6] System informatics, Kobe Univ; [7] Kobe Univ.; [8] EPS, Univ. of Tokyo; [9] Dept. Earth Planet. Sci., Tokyo TECH

The Moon is classified as a nonmagnetized celestial body that does not hold a global, intrinsic magnetic field, and most of the lunar surface is bombarded by the solar wind plasma. Meanwhile, some regions of the lunar surface are locally shielded from the solar wind by magnetic fields of crustal origin. The interaction between the lunar crustal magnetic fields and the solar wind is an important topic relevant to the plasma environment around the Moon. However, it remains unclear how the magnetic field strength on the dayside lunar surface varies globally as a result of the interaction between the lunar crustal magnetic fields and the solar wind.

The global distribution of crustal magnetic field strength has been investigated by electron reflectometry, which remotely infers the surface magnetic field strength from the loss cone angle of reflected electrons from the lunar crustal magnetic field.

As the aim of the conventional electron reflectometry is measurements of the strength of the lunar crustal magnetic field itself, a standard practice is to use data obtained on the night side of the Moon and within the terrestrial magnetotail lobes with less influence of the solar wind plasma. Here we apply the electron reflectometry to the data obtained on the day side of the Moon in the solar wind, thereby investigating variations of the surface magnetic field strength caused by the interaction with the solar wind.

We utilized data obtained by the electron spectrum analyzers (MAP-PACE-ESA) and magnetometer (MAP-LMAG) on board Kaguya. We generated a surface magnetic field strength map by analyzing electron pitch angle distributions measured when the day side lunar surface was exposed to the solar wind. As a result, we obtained a map showing stronger surface magnetic fields than those on the pure crustal field map obtained by the conventional electron reflectometry. This suggests that the lunar crustal magnetic fields are compressed by the solar wind plasma. We will discuss the solar wind dynamic pressure control of the lunar surface magnetic field intensity.

月は、全球的な固有磁場を保持しない非磁化天体に分類され、月面の大部分は地球磁気圏内に存在する時期以外は太陽風に曝されている。一方で、月面には地殻起源の磁場によって太陽風から局所的にシールドされている地域も存在する。このような月地殻磁場と太陽風の相互作用を理解することは、月周辺プラズマ環境の全容を解明するために重要である。ところが、月の昼側において月地殻磁場と太陽風の相互作用により、月面での磁場強度が全球的にどのように変化するかは明らかになっていない。

地殻磁場強度の月面分布は電子反射法を用いて調査されてきた。電子反射法は、月地殻磁場によって反射された電子のロスコーン角から月面での磁場強度を遠隔計測する手法である。従来の電子反射法では、月地殻磁場自体の強度を計測するために、太陽風プラズマの影響が少ない月の夜側や地球磁気圏尾部ローブ内で得られたデータが用いられてきた。今回は、太陽風中で月の昼側で得られたデータに電子反射法を応用することで、太陽風との相互作用によって月面磁場強度がどのように変動するかを調べる。

本研究では、月探査衛星「かぐや」に搭載された電子分析器 MAP-PACE-ESA-S1、-S2 と磁場観測装置 MAP-LMAG によって取得されたデータを用い、月地殻磁場により反射された太陽風電子について解析を行った。昼側月面が太陽風に曝されている時に計測された電子ピッチ角分布を解析し、月面磁場強度マップを作成した。その結果、従来の電子反射法で得られた地殻磁場自体の月面磁場強度マップよりも強い磁場強度を示すマップが得られた。これは太陽風プラズマにより月面地殻磁場が圧縮されていることを示唆している。本発表ではさらに、月面磁場強度の太陽風動圧への依存性について議論する。

かぐや搭載MAP-PACEによる超低高度における月プラズマの観測

齋藤 義文 [1]; 西野 真木 [2]; 横田 勝一郎 [3]; 綱川 秀夫 [4]
[1] 宇宙研; [2] 名大 ISEE; [3] 阪大; [4] 東工大・理・地惑

Observation of Moon Plasma at Very Low Altitude by MAP-PACE on Kaguya

Yoshifumi Saito[1]; Masaki N Nishino[2]; Shoichiro Yokota[3]; Hideo Tsunakawa[4]
[1] ISAS; [2] ISEE, Nagoya University; [3] Osaka Univ.; [4] Dept. Earth Planet. Sci., Tokyo TECH

MAgnetic field and Plasma experiment - Plasma energy Angle and Composition Experiment (MAP-PACE) on Kaguya observed low energy charged particles around the Moon. Kaguya made observation at 100 km altitude polar orbit around the Moon between December 2007 and December 2008. The orbit was lowered to ˜50 km altitude between January 2009 and April 2009, and some orbits had a lower perilune altitude of ˜10 km after April 2009 until Kaguya impacted the Moon on 10 June 2009. One day before Kaguya impacted the Moon, the perilune altitude became lower than 10km. During this time period, Kaguya was in the Earth's magnetosheath

The detailed plasma structure of the magnetic anomaly on the dayside of the Moon was investigated using Kaguya MAP-PACE data. When Kaguya flew over strong magnetic anomalies in the solar wind, deceleration of the solar wind ions, acceleration of the solar wind electrons, and heating of the ions reflected by magnetic anomalies were observed. Deceleration of the ions and acceleration of the electrons were explained by the existence of the DC electric field over dayside magnetic anomalies generated by the difference in the motion between incident electron and ions. Although it was found that the reflected ions had higher temperature and lower energy than the incident solar wind ions and it clearly indicated the existence of a non-adiabatic interaction between solar wind ions and lunar magnetic anomalies, the detailed heating mechanism has remained unsolved. Since the observation at the lower altitude than 10km may give us additional information to understand this heating mechanism, we have analyzed the data obtained at very low altitude <10km around the magnetic anomalies. In addition to the deceleration of the ions and acceleration of the electrons, ion and electron data show more complicated plasma structure than the structure observed at higher altitude.

かぐや搭載MAP-PACEは月周回軌道において、低エネルギーの荷電粒子を計測した。かぐやは2007年12月から2008年12月までの約1年間高度100kmの極軌道で観測を行なった後、2009年1月から4月まで高度を下げて50km高度での観測を行なった。その後、かぐやが2009年6月10日に月面に衝突するまでの間、近月点が10km近くの低高度になることもあったが、特にかぐやが月面に衝突する1日前からは、近月点が10km以下の高度になった。この時期、月は地球磁気圏のマグネトシース領域に位置していた。

月昼間側の磁気異常周辺のプラズマの構造については、MAP-PACEによる観測データを用いてその詳細な構造が明らかになっている。月が太陽風中にあり、かぐやが強い磁気異常の上空を通過する際、太陽風イオンの減速と、電子の加速、そして、月面近くで反射して衛星高度まで戻ってきたイオンが観測された。イオンの減速と、電子の加速は、イオンと電子の運動が異なることによって磁気異常上空で生成された電場で説明することができる。一方、月面近くで反射して衛星高度まで戻ってきたイオンは、エネルギーは入射時より低下し、温度が入射時に比べて高くなっていることも明らかとなった。しかしながら、その加熱のメカニズムは未だに明らかにはなっていない。月高度10kmより低い高度で得られた観測データを解析することによって、イオンの加熱に関する新しい情報を得ることを目的に、かぐやが月面に衝突する1日前の超低高度における磁気異常周辺のデータを調べたところ、より高高度で観測されたイオンの減速と、電子の加速だけでなく、より複雑な構造を示すデータが観測されていることが明らかになってきたため、その結果を報告する。

熱史と整合的なダイナモモデリングを用いた月磁場の進化に関する予備的研究

兵藤 史 [1]; 高橋 太 [2]; 清水 久芳 [3]; 綱川 秀夫 [4]
[1] 九大・理・地惑; [2] 九大・理・地惑; [3] 東大・地震研; [4] 東工大・理・地惑

A preliminary study on a lunar magnetic field evolution using dynamo modeling consistent with a thermal history

Fumi Hyodo[1]; Futoshi Takahashi[2]; Hisayoshi Shimizu[3]; Hideo Tsunakawa[4]
[1] Earth and Planetary Sciences, Kyushu Univ.; [2] Kyushu Univ.; [3] ERI, University of Tokyo; [4] Dept. Earth Planet. Sci., Tokyo TECH

The Moon has no global magnetic field at present unlike the Earth, whereas there are localized crustal magnetic fields, called the lunar magnetic anomalies [Tsunakawa et al., 2015]. Lunar rocks recorded a magnetic field of 4.25 to 3.56 Ga, which is almost the same strength as that on the surface of the Earth [Weiss et al., 2014]. Thus, it is likely that the Moon once had a magnetic field by a dynamo action in its fluid core like the Earth in the past.

In order to investigate how the lunar dynamo worked and evolved with time, we use dynamo modeling changing core geometry [Heimpel et al., 2005]. Here, we assume that the lunar dynamo is driven by compositional convection due to the rejection of light elements from the inner core upon core crystallization. It is noted that the Rayleigh number and the Ekman number should vary with time according to thermal history of the core. We use a one-dimensional thermal history model of the lunar core to have these non-dimensional parameters as a function of inner core size. Throughout this study, we adopt the fixed values of the compositional and magnetic Prandtl numbers at 1, and 3. We discretely change the inner core radius relative to the outer core from 0.1 to 0.7, guided by seismic observations [Weber et al., 2011]. The Ekman number is typically of the order of 10^{-4}. Then, we investigate how dynamo properties vary with inner core growth at various values of the Rayleigh number.

Preliminary calculation results show that when the magnetic field is maintained, the maximum strength of the magnetic field tends to occur at relative inner core size of 0.4. This result is consistent with an argument by a previous study [Heimpel et al,. 2005].

現在，月は地球のようなグローバルな磁場を持たないが，月の地殻には磁気異常と呼ばれる局所的な磁場が存在する [Tsunakawa et al., 2015]．月の岩石には，4.25-3.56 Ga の磁場が記録されており，これは地球磁場と同程度の強度である [Weiss et al., 2014]．よって，過去には，月は地球のように流体コアのダイナモ作用による磁場を持っていた可能性が高い．

月のダイナモが時間とともにどのように生じ進化したのかを調べるために，我々はコアのジオメトリを変化させるダイナモモデリング [Heimpel et al., 2005] を用いる．ここで，月ダイナモは，コアが固化する際に内核から軽元素が追い出されることに起因する組成対流によって駆動されていると仮定する．レイリー数とエクマン数が，コアの熱史に従って時間とともに変化すべきであることに留意し，これら 2 つの無次元パラメータを内核サイズの関数として得るために，月コアの 1 次元熱史モデルを用いている．本研究を通して，組成プラントル数は 1，磁気プラントル数は 3 に固定する．外核半径に対する内核半径の大きさは，月震の観測 [Weber et al., 2011] を目安にして 0.1 から 0.7 まで離散的に変化させる．エクマン数は 10^{-4} のオーダーである．この条件の下で，様々なレイリー数の値の場合に，ダイナモの特性が内核成長とともにどのように変化するかを調べる．

予備的計算の結果は，磁場が維持されている場合には，内核サイズが 0.4 のとき磁場強度が最大になる傾向があることを示している．これは，先行研究 [Heimpel et al,. 2005] での主張と整合性がある．

木星圏探査機JUICE搭載レーザ高度計（GALA）の科学目標

木村 淳 [1]; 鎌田 俊一 [2]; 松本 晃治 [3]; 塩谷 圭吾 [4]; 竝木 則行 [3]; 小林 正規 [5]; 荒木 博志 [3]; 野田 寛大 [3]; 石橋 高 [6]; Hussmann Hauke[7]; Lingenbauber Kay[7]; Oberst Juergen[8]; JUICE レーザ高度計チーム 木村 淳 [9]
[1] 阪大・理・宇宙地球; [2] 北大・創成; [3] 国立天文台; [4] 宇宙研; [5] 千葉工大; [6] 千葉工大; [7] DLR; [8] DLR Institute of Planetary Research; [9] -

Science Objectives of the Ganymede Laser Altimeter (GALA) for the JUICE mission

Jun Kimura[1]; Shunichi Kamata[2]; Koji Matsumoto[3]; Keigo Enya[4]; Noriyuki Namiki[3]; Masanori Kobayashi[5]; Hiroshi Araki[3]; Hirotomo Noda[3]; Ko Ishibashi[6]; Hauke Hussmann[7]; Kay Lingenbauber[7]; Juergen Oberst[8]; Jun Kimura JUICE/GALA Team[9]
[1] Earth & Space Science, Osaka Univ.; [2] Creative Res. Inst., Hokkaido Univ.; [3] NAOJ; [4] JAXA/ISAS; [5] Chiba Institute of Technology/PERC; [6] Chitech/PERC; [7] DLR Institute of Planetary Research; [8] DLR Institute of Planetary Research; [9] -

The JUpiter Icy Moons Explorer (JUICE), led by European Space Agency, has started development toward launch in 2022 (arrival at Jupiter in 2029, and Ganymede orbit insertion in 2032), and we are now developing the GALA instrument onboard JUICE spacecraft collaborating with German Aerospace Center (DLR) and other institutions in Europe. GALA will acquire the key information for understanding the evolution of Jovian icy moons and to play an essential role in the JUICE's purpose: exploration of deep habitat.

Jovian icy moon Ganymede, which is the largest moon in the Solar System and the primary target of the JUICE, can be said to be one of the typical solid bodies along with terrestrial planets in terms of its size and the intrinsic magnetic field originated from the metallic core. However, current knowledge provided by previous explorations is extremely limited since it comes from only several fly-bys. The JUICE will unveil the whole picture of Ganymede by the first orbiting in the history around extra-terrestrial moon. Expected new big picture of the origin and evolution of Ganymede will not only be a key to unveil the origin of diversity among the Solar System bodies, but also contribute to an understanding of exoplanets with a wide diversity.

The GALA will measure a distance between the spacecraft and the surface of icy moons and acquire the topography data (globally for Ganymede, and fly-by region for Europa and Callisto). It will be a first-ever laser altimetry for the icy object. Such information makes surface geologies clear and tremendously improves our understanding of the icy tectonics. By comparing their tectonic styles on the rocky planets/moons, GALA data leads to reconsider the Earth's plate tectonics. In addition, the GALA will confirm a presence/absence of the subsurface ocean by measuring tidal and rotational response, and the gravitational information reflecting the interior structure will be greatly improved. Furthermore, strength and wave-form of reflected laser pulse have an information about surface reflectance at the laser wavelength and small-scale roughness. Finally, we can see degrees of erosion and space weathering without being affected by illumination condition through GALA measurements.

In order to interpret and understand such measurements, accumulated studies for the Earth over the years will be effectively utilized: e.g., the data for surface topography, roughness and albedo will lead to describe the icy tectonics through the knowledge from terrestrial glaciology and experiments on impact and deformation process. The tidal measurements by GALA will also be a window to see its interior based on our knowledge and experiences cultivated through the past geodetic observations, e.g., the SELENE mission for the terrestrial Moon.

Characterization of the icy moons will be achieved not only from the GALA measurements but also synergy of other scientific instruments onboard JUICE spacecraft, for examples, surface images taken by optical camera (JANUS) will confirm the position of GALA laser footprint to complement the point data of GALA for precise topographic mapping. A radar sounder (RIME) and a radio science experiment (3GM) probe the interior structure, especially interior of the icy crust to figure out an occurrence of tectonic features. A visible and infrared imaging spectrometer (MAJIS), an ultraviolet imaging spectrograph (UVS) and a sub-millimeter wave instrument (SWI) will acquire a surface and atmosphere compositional data. A magnetometer (J-MAG) monitors moons' inductive response to the Jovian magnetic field and probes the subsurface ocean with the help of a particle environment package (PEP) and a radio and plasma wave investigation (RPWI). The GALA works closely together with these instruments and plays a leading and a supporting role to clarify the whole picture of Ganymede and other icy moons.

欧日の協同体制で準備が進められている木星氷衛星探査計画 JUICE（2022 年打ち上げ，2029 年木星系到着，2032 年ガニメデ周回軌道投入）において，我々はドイツ航空宇宙センター（DLR）などと協力してレーザ高度計 GALA の開発を進めている．GALA は，JUICE 探査機から標的の天体表面へとレーザを発射し，表面で反射し探査機へ戻ってくるまでの時間を計ることで距離を測定（レーザ測距）する．これによって，天体表面の詳細で定量的な起伏の情報や，天体全体の形状とその時間変化を測ることができる．こうした観測を通して，GALA は「JUICE が掲げる『生命居住可能領域の探査』の本質的役割を担い，氷に支配された天体の進化の解明に不可欠な情報を史上初めて獲得する」ことを目指している．

JUICE の主ターゲットは，木星系最大にして太陽系最大の衛星，ガニメデである．ガニメデは，水星を超える惑星級のサイズ，衛星唯一の金属核起源の固有磁場，大規模なテクトニクス，そして地下海の存在可能性などを持つ点で，氷天体が持ち得る多様な特徴を併せ持つ代表的な存在と言えるが，過去の数回のフライバイ探査にとどまる知見は極めて

限定的である．JUICE は，史上初めての（地球の月以外の）衛星周回探査を行うことによってガニメデの全容を把握し，見出される起源と進化の描像は太陽系内天体の多様性の起源を紐解く鍵となるだけでなく，太陽系内天体の認識に根ざした従来の概念を覆す，多様な系外惑星の理解にも大きな寄与を果たす．

GALA による観測は，氷天体に対する世界初のレーザ測距となる．ガニメデでは周回軌道からの全球測定，エウロパおよびカリストではフライバイに伴う測定を行う．これにより，多様な地形形態とそれらの分布が把握でき，氷衛星の地質活動（氷テクトニクス）の理解が飛躍的に進展するだけでなく，その活動様式をケイ酸塩鉱物でのそれと対比することで，地球のプレート・テクトニクスの再考察にも繋がる．また，木星との潮汐応答（変形や回転変動）の測定を通して地下海の存否が判別できるほか，内部構造に関わる因子の精度が大きく向上する．さらに反射パルスの強度と形状は，レーザ波長での表面反射率や 10 m 規模の粗度を反映するため，表面の風化侵食の程度や組成の情報を，日射角などの観測条件に依存しないデータとして得ることができる．こうした観測と理解の過程には，地球における長年の研究の蓄積が活かされることは言うまでもない．例えば GALA が得る表面地形や粗度・アルベドのデータは，地球の極域や氷河に関する雪氷学や衝突・変形実験などによって得られた知見を通して氷テクトニクスの描像へと繋がる．また潮汐に関するデータは，地球や月（かぐや），小惑星（はやぶさ 1, 2）を対象に長年培われた測地学を基盤として，氷衛星の内部を見通す窓となる．

GALA の観測が直接的にもたらす氷テクトニクス，表面組成，そして地下海など内部構造に関する情報は，他の搭載機器からも多角的な視点で考察を得ることができる．例えば，カメラ（JANUS）が得る画像データは GALA の計測位置を特定し，点の情報を面的な表面地質の理解へと繋げる最も重要な連携機器である．氷層を透過するレーダの RIME や重力場測定を行う 3GM は地質の産状や内部構造の把握に寄与し，可視・近赤外撮像分光計（MAJIS）や紫外撮像分光計（UVS），サブミリ波観測器（SWI）は，様々な波長で表層の組成に関する情報を得る．磁力計（J-MAG）は木星磁場の変動に伴う衛星の電磁感応をモニターし，プラズマ環境観測パッケージ（PEP）や電波・プラズマ波動観測器（RPWI）による観測のサポートを得て地下海の規模や組成（電気伝導度）を制約する．このように GALA が得る観測データは，他機器が取得するデータと密接に関係し合い，それらの科学目標の基盤あるいはサポート的役割を担う．

Feasibility study of passive subsurface radar using waveform data of Jovian decametric radiation

Atsushi Kumamoto[1]; Fuminori Tsuchiya[2]; Tomoki Kimura[3]; Yasumasa Kasaba[4]; Hiroaki Misawa[5]; Walter Puccio[6]; J.-E. Wahlund[6]; Baptiste Cecconi[7]; Wlodek Kofman[8]
[1] Dept. Geophys, Tohoku Univ.; [2] Planet. Plasma Atmos. Res. Cent., Tohoku Univ.; [3] Tohoku University; [4] Tohoku Univ.; [5] PPARC, Tohoku Univ.; [6] IRF-U; [7] LESIA, Observatoire de Paris; [8] CNRS IPAG Grenoble

Feasibility study of passive subsurface radar has been performed using waveform data of Jovian decametric radiation obtained in ground-based observations at Tohoku University Observatory.

In Jupiter Icy Moon Explorer (JUICE) mission, we are planning passive subsurface radar observations of Jupiter's icy moons by using Radio and Plasma Wave Investigation (RPWI), passive receiver covering wide frequency range from 80 kHz to 45 MHz, in addition to Radar for Icy Moon Exploration (RIME), the active radar operated at frequency of 9 MHz.

In passive subsurface radar observations, Jovian decametric (DAM) and hectometric (HOM) emissions are utilized as radar the pulse. By detecting echoes of Jovian radio emissions reflected at the permittivity contrasts on and below the Jovian icy moon's surface, we can measure the surface and subsurface structures of the ice crust of the Jovian icy moons. The echoes can be detected in two methods: (1) Applying auto-correlation analysis to waveform data [Romero-Wolf et al., 2015], and (2) Measuring interference patterns in spectrogram [Kumamoto et al., 2017]. If the duration of the coherence of Jovian radio emissions is shorter than 2ms, round-trip propagation time of radio waves between the spacecraft and icy moon's surface, the former method will be effective. Otherwise, the latter method will be effective.

In this study, we generate simulated data from the waveform data obtained in ground-based observations at Tohoku University Observatory. In order to simulate the surface and subsurface echoes, delayed waveform was added to the observed waveform. Then we performed following analyses with simulated waveform data: (1) The waveform data was divided into 4096-point subsets. (2) Power spectrum was obtained by applying FFT to divided waveforms. (3) Auto-correlation function was obtained by applying FFT to the power spectrum. Finally, we checked interference patterns in the power spectrum and delayed components in auto-correlation function. We could identify subsurface echo component in interference in spectrogram and in auto correlation function if the subsurface echo intensity with respect to surface echo is larger than -30dB. In onboard data processing of RPWI, the raw waveform is divided into those in multiple sub-bands with a bandwidth of 296 kHz. The test of onboard data processing with simulated waveform data will also be reported in the presentation.

High dynamic-range observation using a low-scattered light telescope PLANETS: feasibility study

Masato Kagitani[1]; Takeshi Sakanoi[2]; Yasumasa Kasaba[3]
[1] PPARC, Tohoku Univ; [2] Grad. School of Science, Tohoku Univ.; [3] Tohoku Univ.

High dynamic-range (HDR) observation is one of the key technique to reveal composition, distribution and dynamics of plasma and neutrals in the vicinity of planets and their moons in our solar system, e.g. water plumes on Europa and Enceladus, volcanic plumes on Io, escaping plasma and neutrals from Venus and Mars, and so on. A low-scattered light telescope, PLANETS (Polarized Light from Atmospheres of Nearby Extra-Terrestrial Systems) would be an 1.8-m off-axis telescope on Mt. Haleakala, Hawaii under collaboration with Japan, USA, Germany, Brazil, and France. The off-axis optical system enables us to achieve HDR measurements without diffraction by support structure of secondary mirror. We present feasibility study of monitoring water plumes on Europa, neutral torus close to Enceladus, and ionosphere on Mars using PLANETS telescope.

To test feasibility of HDR under actual condition of wavefront error which includes by an optical system as well as by atmospheric turbulence, modeling the propagation of light though the system was made based on Fraunhofer (far-field) calculations with help from PROPER library (Krist 2007). The optical system consists of an entrance pupil (1.85 m), primary mirror, a deformable mirror, an occulting mask, a Lyot mask on a pupil, and a detector on image plane. We gave wavefront error made by atmospheric turbulence (typical Fried length is 15 cm) and the optical system represented with power spectral density. Then, dynamic range of point spread function was calculated for several cases of surface roughness of the primary mirror, 1 to 8 nm r.m.s., and number of control points for active wavefront compensation by a deformable mirror, 7 to 24. Finally we calculated brightness distribution of background continuum, and derived signal-to-noise ratio for each observing target assuming expected brightness and band-width of spectroscopy. For $O_2{}^+$ 561 nm and $N_2{}^+$ 391 nm emissions from Martian ionosphere and O 630 nm emission from Enceladus torus, sufficient signal-to-noise ratio is expected for 2-hour integration by employing wavefront compensation with 7x7 deformable mirror and small roughness of primary mirror, 2-nm r.m.s. Whereas for O 630 nm emissions from water plumes on Europa, wavefront compensation by 24x24 deformable mirror is needed to achieve sufficient signal-to-noise ratio for 2-hour integration. Now the primary mirror is waiting for final polishing. We will present required surface error of the primary as well as a concept design of an active support structure to fulfill the requirement.

惑星探査用飛行時間計測型中性粒子質量分析器の開発

福山 代智 [1]; 斎藤 義文 [2]; 浅村 和史 [3]; 横田 勝一郎 [4]
[1] 東大・理・地球惑星; [2] 宇宙研; [3] 宇宙研; [4] 阪大

Development of a neutral particle TOF-MS for future planetary explorations

Daichi Fukuyama[1]; Yoshifumi Saito[2]; Kazushi Asamura[3]; Shoichiro Yokota[4]
[1] Earth and Planetary Science, The University of Tokyo; [2] ISAS; [3] ISAS/JAXA; [4] Osaka Univ.

In-situ material measurement in planetary exploration is quite important in understanding the evolution of the planets and their atmosphere. For the purpose of performing in-situ elemental analysis, mass spectrometers were installed, for example, on NASA's Curiosity rover and the ESA's Rosetta spacecraft. In Japan, however, we still do not have a neutral particle mass spectrometer for the future planetary exploration. Therefore, we have decided to develop a neutral particle Time Of Flight Mass Spectrometer (TOF-MS) aiming at using for the future planetary exploration.

Incident neutral particles into TOF-MS are ionized for the further analysis of mass identification. The effects of the initial position and initial energy of the ionized ions on the mass analysis should be minimized to get a fine mass resolution. We decided to adopt two-stage acceleration and single-stage reflector. From the analytical solution obtained on the condition that the TOF converges regardless of the variation of the initial position and energy of ions, we have optimized the size and potential of the electrodes in the instrument. We are now trying to improve the performance of the prototype TOF-MS with two-stage acceleration and single-stage reflector.

In parallel with improving the performance of the prototype TOF-MS, we are developing a multi-reflector type TOF-MS which has the potential to increase mass resolution under the size constraint. Compared to the single-reflector type TOF-MS, the flight path becomes about three times longer which makes the mass resolution of the TOF-MS improved. However, as the flight length increases, effects of variations in the flight path of the ions increase and the detection rate decreases. Therefore we have to determine the analytical solution in order to identify the parameters that control the performance and carefully optimize the size and voltages of the multi-reflector TOF-MS by using a software that simulates the particle motion in the instrument.

We will report on the test results of the prototype TOF-MS and the optimized design of the multi-reflector type TOF-MS.

月・惑星探査において、中性大気や月・惑星表面物質のその場での質量分析は、惑星大気の変遷や月・惑星の進化を理解する上で重要である。これまでの多くの惑星探査機には惑星周辺空間で中性粒子を計測するための質量分析器が搭載されてきたほか、近年の太陽系探査において、NASA の火星探査機「Curiosity」や ESA の彗星探査機「Rosetta」には天体表面物質のその場元素分析を行うための質量分析器が搭載されている。しかしながら、日本では中性粒子を計測するための質量分析器の開発が遅れており、将来の惑星探査や月・惑星への着陸探査に向けた開発を加速する必要が高まっている。そこで我々は月・惑星探査を想定した中性粒子質量分析用リフレクトロン型 TOF-MS(Time-Of-Flight Mass Spectrometer: 飛行時間計測型質量分析器) の開発を進めている。

TOF-MS においては装置に取り込んだ中性粒子をイオン化するが、イオンの初期位置や初期エネルギーのばらつきによる質量分解能の低下を抑えるために、イオンを反射させるリフレクター方式を採用している。イオンの初期位置や初期エネルギーのばらつきに依らず飛行時間が収束することを条件にして求めた解析解から装置の寸法や印加電圧等のパラメータの最適値を決定、イオン加速部２段・イオン反射部 1 段構成の試験モデルを設計・製作し、試験・改良を進めている。

並行して、我々は、限られた容積で質量分解能を向上させることを目指し、反射を複数回行うマルチリフレクター型の TOF-MS の開発を行っている。これまでの 1 回反射のリフレクトロンと比較して、３回反射のマルチリフレクター型 TOF-MS はイオンの飛行時間が約３倍となり、分解能の向上が期待される。一方で、イオンの飛行経路はイオンの飛行距離が長くなるにつれて分散するため、検出効率の低下が懸念される。そこで、 1 回反射の TOF-MS の設計と同様に解析解を導出し、計算機シミュレーションによる装置寸法と印加電圧の最適化を慎重に行うことで、装置の総合的な性能を最適化した試験モデルを製作する準備を進めている。

本発表ではこれまで改良を進めてきた 1 回反射 TOF-MS 試験モデルの性能試験の結果と、マルチリフレクター型 TOF-MS の最適化設計について報告する。

周回機搭載質量分析器による遠隔での天体表面組成分析手法の開発

横田 勝一郎 [1]; 寺田 健太郎 [2]; 齋藤 義文 [3]; 加藤 大羽 [4]; 西野 真木 [5]; 綱川 秀夫 [6]
[1] 阪大; [2] 広大・理・地惑システム; [3] 宇宙研; [4] 東大・理・地惑; [5] 名大 ISEE; [6] 東工大・理・地惑

Development of a remote analysis of small bodies' surface by a mass spectrometer on orbiters

Shoichiro Yokota[1]; Kentaro Terada[2]; Yoshifumi Saito[3]; Daiba Kato[4]; Masaki N Nishino[5]; Hideo Tsunakawa[6]
[1] Osaka Univ.; [2] Isotope geochemistry, Hiroshima Univ.; [3] ISAS; [4] EPS, Univ. of Tokyo; [5] ISEE, Nagoya University; [6] Dept. Earth Planet. Sci., Tokyo TECH

Lander and rover explorations which have considerably succeeded in measuring the planetary surface materials need large costs and risks in their developments and operations, compared to orbiter missions. We aim at developing an isotope mass analysis method of small bodies' sur-face by measuring secondary ions emitted by the solar wind bombardment. The analysis tech-nique can be used for previous observations before landing.

In Japan, a number of spaceborne mass spectrometers and orbiters have been developed and observed planetary particles while lander and rover explorations have just started. For example, Kaguya, a lunar obiter, succeeded in measuring secondary ions emitted from the lunar surface. This means that the remote analysis of small bodies' surface by orbiters might be possible. We estimated secondary ion fluxes by using the Kaguya observation data of 1.5 years to develop the analysis technique. Comparing the laboratory experiment data using ion beam and a numeri-cal model of SDTrimSP, we have investigated the mechanism of the secondary ion emission by the solar wind. The results of this study will be utilized for future planetary exploration missions such as MMX(Martian Moons eXploration).

着陸機探査によって天体表面組成分析において著しい成果が出されているが、着陸機探査は周回機探査に比べると開発や観測運用においてコストとリスクが大きくなる。我々は、太陽風照射によって発生する天体起源二次イオンの計測により周回軌道上から遠隔で天体表面の質量同位体分析を行う手法の確立を目指している。これは着陸探査に対して事前の補完的な観測手法にも成りうる。

日本の着陸機探査は始まったばかりであるが、周回探査機による科学観測では日本でも多くの実績があり、その中で宇宙（惑星磁気圏）プラズマ物理研究を目指した宇宙機用プラズマ観測器はいくつも開発されている。例えば、月周回探査「かぐや」搭載の質量分析器では月の表面から発生したイオンが観測された。月のように大規模な大気・固有磁場を持たない小型天体では、太陽風の直接照射によって表面から二次イオンが発生すること（スパッタリング）が室内実験等で知られている。「かぐや」による月起源イオン観測は、実績有る技術だけで小型天体表面物質の遠隔同位体質量分析が可能であることを示している。

太陽風による二次イオン放出の特性を検証して汎用的な表面物質情報を得る解析手法を確立することを目指し、「かぐや」のプラズマ観測データを利用して太陽風によって発生する天体表面起源二次イオンフラックスの評価を行った。「かぐや」では太陽風や UV の直接照射を受ける月周辺のプラズマ環境が 1.5 年観測されている。質量分解能 M/M ～20 は重イオンの分別に十分ではないが、月面物質を構成する金属イオン相当のカウントは得られている。観測データから太陽風パラメータに対応した二次イオン放出率を求めて、周回軌道上でのイオン観測から月面組成比を導出する手法について考察する。スパッタリング現象として見る場合、太陽風のエネルギー帯（～1 keV）では実験室プラズマで典型的な高エネルギー領域（>10s keV）と比較してモデル化が遅れている。追加のスパッタリング実験や、最近のスパッタリングモデル（SDTrimSP）を利用して、太陽風による天体表面での二次イオン放出のモデル化に迫る。本発表では、「かぐや」観測データから得られた月面組成を紹介し、二次イオンを用いた月表面の「天然」SIMS 分析について評価する。本研究成果は火星衛星探査計画 MMX 等の将来月惑星探査への展開を考えている。

MMO搭載MIAのトップハット分析器特性のわずかな非対称性について

三宅 亙 [1]; 齋藤 義文 [2]; 横田 勝一郎 [3]
[1] 東海大・工; [2] 宇宙研; [3] 阪大

On slight asymmetry of analyzer characteristics of MIA onboard Mercury Magnetospheric Orbiter

Wataru Miyake[1]; Yoshifumi Saito[2]; Shoichiro Yokota[3]
[1] Tokai Univ.; [2] ISAS; [3] Osaka Univ.

MIA (Mercury Ion Analyzer) on board MMO employs a top-hat electrostatic analyzer, which has axisymmetric toroidal electrodes and is designed to have no dependence in its characteristics on azimuthal direction of incident ions. However, our ground calibration experiments have revealed that it has a slight dependence. We have tried to explain the dependence by means of three dimensional model calculations. We assumes that all parts of electrode are manufactured precisely. Our first results shows that a slight relative shift of electrodes with no rotation alone cannot explains the energy and g-factor characteristics consistently. We are next trying to introduce relative rotation (tilt) between electrodes in our model calculations.

水星磁気圏探査機 MMO に搭載された MIA（水星イオン分析器）には軸対象なトップハット型静電分析器が使われている。その軸対称性故に、この分析器は入射イオンの方位角には依存性を持たないはずであるが、地上試験ではわずかな依存性を持つことが確認された。その原因として、個々のパーツは正確に製造されているが、その組上げにおいて取り付け誤差があるため、との仮定おいて、ずれを取り入れた３次元のモデル計算を繰り返してきた。その結果、パーツの相互の平行移動だけでは特性（感度、エネルギー）の入射方位角依存性が説明できないことが明らかとなってきた。本発表では、残された可能性の１つとしてパーツの回転（傾き）を取りいれたモデル計算による検討を紹介する。